PHYSICAL REVIEW C **80**, 014612 (2009)

Hard breakup of two nucleons from the ^{3}He nucleus

Misak M. Sargsian and Carlos Granados
Florida International University, Miami, Florida 33199, USA
(Received 20 January 2009; revised manuscript received 23 June 2009; published 31 July 2009)

We investigate a large angle photodisintegration of two nucleons from the ^{3}He nucleus within the framework of the hard rescattering model (HRM). In the HRM a quark of one nucleon knocked out by an incoming photon rescatters with a quark of the other nucleon leading to the production of two nucleons with large relative momentum. Assuming the dominance of the quark-interchange mechanism in a hard nucleon-nucleon scattering, the HRM allows the expression of the amplitude of a two-nucleon breakup reaction through the convolution of photon-quark scattering, NN hard scattering amplitude, and nuclear spectral function, which can be calculated using a nonrelativistic ^{3}He wave function. The photon-quark scattering amplitude can be explicitly calculated in the high energy regime, whereas for NN scattering one uses the fit of the available experimental data. The HRM predicts several specific features for the hard breakup reaction. First, the cross section will approximately scale as s^{-11}. Second, the s^{11} weighted cross section will have the shape of energy dependence similar to that of s^{10} weighted NN elastic scattering cross section. Also one predicts an enhancement of the pp breakup relative to the pn breakup cross section as compared to the results from low energy kinematics. Another result is the prediction of different spectator momentum dependencies of pp and pn breakup cross sections. This is due to the fact that the same-helicity pp-component is strongly suppressed in the ground state wave function of ^{3}He. Because of this suppression the HRM predicts significantly different asymmetries for the cross section of polarization transfer NN breakup reactions for circularly polarized photons. For the pp breakup this asymmetry is predicted to be zero while for the pn it is close to $\frac{2}{3}$.

DOI: 10.1103/PhysRevC.80.014612 PACS number(s): 24.85.+p, 25.10.+s, 25.20.−x

I. INTRODUCTION

Two-body breakup processes involving nuclei at high momentum and energy transfer play an important role in studies of nuclear QCD. The uniqueness of these processes is in the effectiveness by which large values of invariant energy are produced at rather moderate values of beam energy. The kinematics of two-body photodisintegration provide the relation

$$s_{\gamma NN} \approx 4m_N^2 + 4E_\gamma m_N, \tag{1}$$

in which the produced invariant energy grows with the energy of the probe twice as fast as compared, for example, to hard processes involving two protons, in which case $s_{NN} = 2m_N^2 + 2E \cdot m_N$. As it follows from Eq. (1), already at photon energies of 2 GeV the produced invariant mass on one nucleon, $M \sim \sqrt{\frac{S_{\gamma NN}}{2}}$, exceeds the threshold at which deep-inelastic processes become important, $M \gtrsim 2$ GeV.

Combining the above property with a requirement that the momentum transfer in the reaction exceeds the masses of the particles involved in the scattering ($-t, -u \gg m_N^2$) one sets into a hard scattering kinematic regime, in which case we expect that only minimal Fock components dominate in the wave function of the particles involved in the scattering. Assuming that all the constituents of the minimal Fock component participate in a hard scattering one arrives at the constituent-counting rule [1,2]. According to this rule we are able to predict the energy dependence of any hard processes at fixed and large center of mass (c.m.) scattering angles. For example, for the $A + B \to C + D$ hard scattering process the constituent-counting rule predicts the following energy dependence for the scattering amplitude:

$$\mathcal{M} \approx s^{-\frac{n_A+n_B+n_C+n_D-4}{2}}, \tag{2}$$

with

$$\frac{d\sigma}{dt} \sim \frac{|\mathcal{M}|^2}{s^2}. \tag{3}$$

In Eq. (2) n_i is the number of constituents in the minimal Fock component of the wave function of particle i involved in the scattering. These predictions were confirmed for a wide variety of hard processes involving leptons and hadrons.

One of the most interesting aspects of the constituent-counting rule is that its application allows us to check the onset of quark degrees of freedom in hard reactions involving nuclei [3,4]. This is essential for probing the quark-gluon structure of nuclei. For example if quarks are involved in hard photodisintegration of the deuteron then according to Eqs. (2) and (3) one expects that $\frac{d\sigma}{dt} \sim s^{-11}$ [3].

During the last decade there were several experiments in which 90° c.m. photodisintegration of the deuteron had been studied at high photon energies [5–12]. These experiments clearly demonstrated the onset of s^{-11} scaling for the differential cross section at 90° c.m., starting at $E_\gamma \geqslant 1$ GeV. Also, the polarization measurements [9,12] were generally in agreement with the prediction of the helicity conservation—a precursor of the dominance of the mechanism of hard gluon exchange involving quarks.

Even though two-body scattering experiments demonstrate clearly an onset of quark degrees of freedom in the reaction, they do not affirm the onset of the perturbative QCD (pQCD) regime. Indeed it has been argued that the validity of constituent-counting rule does not necessarily lead to the

validity of pQCD (see, e.g., Refs. [13,14]). In several measurements in which the constituent quark rule works pQCD still underestimates the observed cross sections sometimes by several orders of magnitude (see, e.g., Refs. [15,16]). The latter may indicate a substantial contribution due to nonperturbative effects, although one still may expect sizable contributions from pQCD due to generally unaccounted hidden color components in the hadronic and nuclear wave functions [17].

A similar situation also exists for the case of hard photodisintegration of the deuteron. Even though experiments clearly indicate the onset of s^{-11} scaling for the cross section of these reactions at 90° c.m., one still expects sizable nonperturbative effects. Theoretical methods of calculation of these effects are very restricted. They use different approaches to incorporate nonperturbative contributions in the process of hard photodisintegration of the deuteron. The reduced nuclear amplitude (RNA) formalism includes some of the nonperturbative effects through the nucleon form factors [18,19], while in the quark-gluon string model (QGS) [20] nonperturbative effects are accounted for through the reggeization of scattering amplitudes. Also recently, large c.m. angle photodisintegration of the deuteron for photon energies up to 2 GeV was calculated within point-form relativistic quantum mechanics approximation [21] in which the strength of the reaction was determined by short range properties of the NN interaction potential.

In the QCD hard rescattering model (HRM) [22,23] it is assumed that the energetic photon knocks out a quark from one nucleon in the deuteron that subsequently experiences hard rescattering with a quark of the second nucleon. The latter leads to the production of two nucleons with large relative momentum. The summation of all the relevant rescattering diagrams results in a scattering amplitude in which the hard rescattering is determined by the large-momentum transfer pn scattering amplitude, which includes noncalculable nonerturbative contributions. Experimental data are used to estimate the hard pn scattering amplitude. The HRM allows us to calculate the absolute cross section of 90° c.m. hard photodisintegration of the deuteron without using additional adjustable parameters.

Also, within the QGS [24] approximation and the HRM [25,26] rather reasonable agreement has been obtained for polarization observables [12].

Although all the above-mentioned models describe the major characteristics of hard photodisintegration of the deuteron they are based on very different approaches in the calculation of the nonperturbative parts of the photodisintegration reaction. To investigate further the validity of these approaches it was suggested in Ref. [27] to extend the studies of high energy two-body photodisintegration to the case of large angle c.m. breakup of two protons from the ^{3}He target. In this case not only do the predictions of the above-described models (RNA, QGS, HRM) for absolute cross section diverge significantly but also the two-proton breakup reaction from ^{3}He provides additional observables such as spectator-neutron momentum distributions that can be used to check further the validity of the models. The analysis of the first experimental data on pp photodisintegration of the ^{3}He nucleus at high momentum transfer is currently in progress at Jefferson Lab [28]. It may significantly advance our understanding of the mechanism of hard breakup reactions involving nuclei.

In the present work we carry out detailed studies of reactions involving hard breakup of both pp and pn pairs from the ^{3}He target. We demonstrate that comparative study of pp and pn breakup processes allows us to gain new insight into the nature of large c.m. angle scattering. One of the observations is that the relative strength of pp to pn breakup is larger than the one observed in low energy reactions. This is related to the onset of quark degrees of freedom in hard breakup reactions in which effectively more charges are exchanged between two protons than between proton and neutron.

Another signature of the HRM is that the shapes of the energy dependencies of s^{11}-scaled differential cross sections of pp and pn breakup reactions mirror the shapes of the energy dependencies of s^{10}-scaled differential cross sections of hard elastic pp and pn scatterings.

Within the HRM one observes also that pp and pn hard breakup processes are sensitive to different components of the ^{3}He ground state wave function. This results in different spectator-nucleon momentum dependencies for pp and pn hard breakup cross sections.

Because of the different ground state wave function components involved in pp and pn breakup reactions, the HRM also predicts significantly different magnitudes for transferred longitudinal polarizations for these two processes.

The article is organized as follows: In Sec. II, within HRM, we present a detailed derivation of the differential cross section of the reaction of hard breakup of two-nucleons from a ^{3}He target. In Sec. III we apply the formulas derived in the previous section to calculate the differential cross section of a proton-neutron breakup reaction, while in Sec. IV calculations are done for a two-proton breakup reaction. Section V considers the relative contribution of two- and three-body processes for hard breakup reactions involving $A \geqslant 3$ nuclei. In Sec. VI we present numerical estimates for differential cross sections of pn and pp breakup reactions. In Sec. VII we discuss the polarization transfer mechanism of the HRM and estimate the asymmetry of the cross section with respect to the helicity of the outgoing proton. Results are summarized in Sec. VIII. In Appendix A the details of the derivation of the hard rescattering amplitude are given. In Appendix B we discuss the quark-interchange contribution to hard NN elastic scattering. Appendix C discusses the method of calculation of quark-charge factors within the quark-interchange mechanism of NN hard elastic scattering. In Appendix D we present the complete list of the HRM helicity amplitudes for high energy two-nucleon breakup of the ^{3}He nucleus.

II. HARD PHOTODISINTEGRATION OF TWO NUCLEONS FROM ^{3}He

A. Reference frame and kinematics

We are considering a hard photodisintegration of two nucleons from the ^{3}He target through the reaction

$$\gamma + {}^3\mathrm{He} \to (NN) + N_s, \tag{4}$$

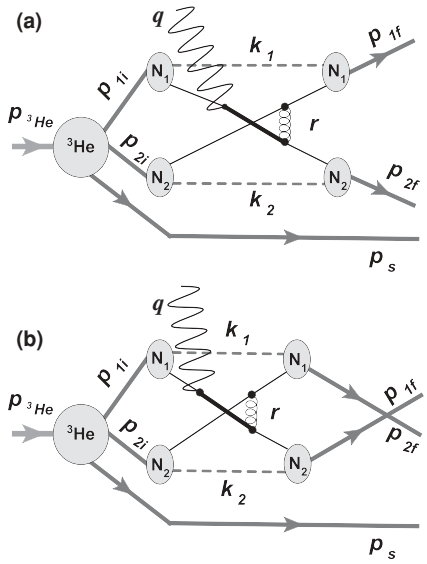

FIG. 1. Typical hard rescattering diagram for the NN photodisintegration from the ^{3}He target.

in which two nucleons (NN) are produced at large angles in the "γ-NN" center of mass reference frame with momenta comparable to the momentum of the initial photon, q (>1 GeV/c). The third nucleon, N_s, is produced with very small momentum $p_s \ll m_N$. (Definitions of four-momenta involved in the reaction are given in Fig. 1.)

We consider "γ-NN" in a "$q_+ = 0$" reference frame, where the light-cone momenta[1] of the photon and the NN pair are defined as follows:

$$q^\mu \equiv (q_+, q_-, q_\perp) = \left(0, \sqrt{s'_{NN}}, 0\right),$$

$$p^\mu_{NN} \equiv (p_{NN+}, p_{NN-}, p_{NN\perp}) = \left(\sqrt{s'_{NN}}, \frac{M^2_{NN}}{\sqrt{s'_{NN}}}, 0\right), \quad (5)$$

where $p^\mu_{NN} = p^\mu_{^3\mathrm{He}} - p^\mu_s$, $M^2_{NN} = p^\mu_{NN} p_{NN,\mu}$, and $s'_{NN} = s_{NN} - M^2_{NN}$. Here the invariants, s_{NN} and t_{NN}, are defined as follows:

$$s_{NN} = (q + p_{NN})^2 = (p_{f1} + p_{f2})^2$$
$$t_{NN} = (q - p_{f1})^2 = (p_{f2} - p_{NN})^2. \quad (6)$$

As it follows from Eq. (5) in the limit of $\frac{M^2_{NN}}{s'_{NN}} \to 0$ the "$q_+ = 0$" reference frame coincides with the center of mass frame of the γ-NN system. As such it is maximally close to the reference frame used for the $\gamma d \to p + n$ reaction in Refs. [22] and [25].

B. Hard rescattering model

The hard rescattering model is based on the assumption that, in the hard two-nucleon photodisintegration reaction, two nucleons with large relative momenta are produced because of the hard rescattering of a fast quark from one nucleon with a quark from the other nucleon. In this scenario the fast quark is knocked out from a low-momentum nucleon in the nucleus by an incoming photon. This approach is an alternative to the models in which it is assumed that the incoming photon breaks the preexisting two-nucleon state, which has very large relative momentum in the nucleus.

The validity of the HRM is based on the observation that the ground state wave functions of light nuclei peak strongly at small momenta of bound nucleons, $p \sim 0$. Thus, diagrams in which an energetic photon interacts with bound nucleons of small momenta will strongly dominate the diagrams in which the photon interacts with bound nucleons that have relative momenta $p \geqslant m_N$.

The resulting scenario that the HRM sketches out is as follows (see, e.g., Fig. 1): first, the incoming photon will knock out a quark from one of the nucleons in the nucleus and then the struck quark that now carries almost the whole momentum of the photon will share its momentum with a quark from the other nucleon through the exchanged gluon. The resulting two energetic quarks will recombine with the residual quark-gluon systems to produce two nucleons with large relative momentum ($\sim q$). This recombination will contain gluon exchanges and also incalculable nonperturbative interactions.

Note that for the quark-gluon picture discussed above to be relevant the intermediate masses m_{int} produced after the photon absorption should exceed the mass scale characteristic for deep inelastic scattering, $W \sim 2.2$ GeV. Using the relation $m_{\mathrm{int}} \approx \sqrt{m_N^2 + 2E_\gamma m_N}$, from the requirement that $m_{\mathrm{int}} \geqslant W$ one obtains the condition $E_\gamma \geqslant 2$ GeV. Additionally, to ensure the validity of quark degrees of freedom in the final state rescattering, one requires $k_{\mathrm{rel}} \geqslant 1$ GeV/c for the relative momentum k_{rel}, of two outgoing nucleons. All of these imposes a restriction on the incoming photon energy, $E_\gamma \geqslant 2$ GeV, and for transferred momenta $-t, -u \geqslant 2$ GeV^2. Note that provided a smooth transition from hadronic to quark-gluon degrees of freedom in nuclei one expects the validity of the HRM to extend to even lower values of E_γ ($\gtrsim$1 GeV). This expectation was confirmed in recent measurements of angular dependencies of the $\gamma d \to pn$ cross section for a wide range of incoming photon energies [11].

To calculate the differential cross section of the hard photodisintegration reaction of Eq. (4) within the HRM one needs to evaluate the sum of hard rescattering diagrams similar to the one presented in Fig. 1. We start with analyzing the scattering amplitude corresponding to the diagrams of Fig. 1. Using Feynman rules and applying the light-cone wave function reduction described in Appendix A, we obtain

$$\langle \lambda_{1f}, \lambda_{2f}, \lambda_s | A | \lambda_\gamma, \lambda_A \rangle$$
$$= \sum_{(\eta_{1f},\eta_{2f}),(\eta_{1i},\eta_{2i}),(\lambda_{1i},\lambda_{2i})} \int \left\{ \frac{\psi_N^{\dagger\lambda_{2f},\eta_{2f}}(p_{2f}, x'_2, k_{2\perp})}{1 - x'_2} \bar{u}_{\eta_{2f}} \right.$$
$$\left. \times (p_{2f} - k_2)\left[-igT_c^F \gamma^\nu\right] \frac{i[\not{p}_{1i} - \not{k}_1 + \not{q} + m_q]}{(p_{1i} - k_1 + q)^2 - m_q^2 + i\epsilon} \right.$$

[1]The light-cone four-momenta are defined as $(p_+, p_-, p_\perp)$, where $p_\pm = E \pm p_z$. Here the z axis is defined in the direction opposite to the incoming photon momentum.

$$\times\left[-iQ_i e\epsilon_\perp^{\lambda_\gamma}\gamma^\perp\right]u_{\eta_{1i}}(p_{1i}-k_1)\,\frac{\psi_N^{\lambda_{1i},\eta_{1i}}(p_{1i},x_1,k_{1\perp})}{(1-x_1)}\Bigg\}_1$$

$$\times\left\{\frac{\psi_N^{\dagger\lambda_{1f},\eta_{1f}}(p_{1f},x_1',k_{1\perp})}{1-x_1'}\,\bar u_{\eta_{1f}}(p_{1f}-k_1)\right.$$

$$\left.\times\left[-igT_c^F\gamma^\mu\right]u_{\eta_{2i}}(p_{2i}-k_2)\,\frac{\psi_N^{\lambda_{2i},\eta_{2i}}(p_{2i},x_2,k_{2\perp})}{(1-x_2)}\right\}_2$$

$$\times G^{\mu,\nu}(r)\frac{dx_1}{x_1}\frac{d^2k_{1\perp}}{2(2\pi)^3}\frac{dx_2}{x_2}\frac{d^2k_{2\perp}}{2(2\pi)^3}$$

$$\times\frac{\Psi_{^3\mathrm{He}}^{\lambda_A,\lambda_{1i},\lambda_{2i},\lambda_s}(\alpha,p_\perp,p_s)}{(1-\alpha)}\frac{d\alpha}{\alpha}\frac{d^2p_\perp}{2(2\pi)^3}-(p_{1f}\longleftrightarrow p_{2f}),\tag{7}$$

where the $(p_{1f}\longleftrightarrow p_{2f})$ part accounts for the diagram in Fig. 1(b). Here the four-momenta, p_{1i}, p_{2i}, p_s, k_1, k_2, r, p_{1f}, and p_{2f}, are defined in Fig. 1. Note that k_1 and k_2 define the four-momenta of residual quark-gluon system of the nucleons without specifying their actual composition. We also define x_1, x_1', x_2, and x_2' as the light-cone momentum fractions of initial and final nucleons carried by their respective residual quark-gluon systems: $x_{1(2)}=\frac{k_{1(2)+}}{p_{1(2)i+}}$ and $x'_{1(2)}=\frac{k_{1(2)+}}{p_{1(2)f+}}$. For the ^{3}He wave function, $\alpha=\frac{p_{2+}}{p_{NN+}}$ is the light-cone momentum fraction of the NN pair carried by one of the nucleons in the pair, and $p_\perp$ is their relative transverse momentum. The scattering process in Eq. (7) can be described through the combination of the following blocks: (a) $\Psi_{^3\mathrm{He}}^{\lambda_A,\lambda_{1i},\lambda_{2i},\lambda_s}(\alpha,p_\perp,p_s)$, is the light-cone ^{3}He wave function that describes a transition of the ^{3}He nucleus with helicity λ_A into three nucleons with λ_{1i}, λ_{2i}, and λ_s helicities, respectively. (b) The term in $\{\cdots\}_1$ describes the "knocking out" of an η_{1i}-helicity quark from a λ_{1i}-helicity nucleon by an incoming photon with helicity λ_γ. Subsequently, the knocked-out quark exchanges a gluon, ($[-igT_c^F\gamma^\nu]$), with a quark from the second nucleon producing a final η_{2f}-helicity quark that combines into the nucleon "$2f$" with helicity λ_{2f}. (c) The term in $\{\cdots\}_2$ describes the emerging η_{2i}-helicity quark from the λ_{2i}-helicity nucleon that then exchanges a gluon, ($[-igT_c^F\gamma^\mu]$), with the knocked-out quark and produces a final η_{1f}-helicity quark that combines into the nucleon "$1f$" with helicity λ_{1f}. (d) The propagator of the exchanged gluon is $G^{\mu\nu}(r)=\frac{d^{\mu\nu}}{r^2+i\varepsilon}$ with polarization matrix, $d^{\mu\nu}$ (fixed by the light-cone gauge), and $r=(p_2-k_2+l)-(p_1-k_1+q)$, with $l=(p_{2f}-p_{2i})$. In Eq. (7) the $\psi_N^{\lambda,\eta}$ represents everywhere an η-helicity single quark wave function of a λ-helicity nucleon as defined in Eq. (A14) and u_τ is the quark spinor defined in the helicity basis.

We now consider the denominator of the struck quark's propagator, which can be represented as follows:

$$(p_{1i}-k_1+q)^2-m_q^2+i\varepsilon=(1-x_1)s'_{NN}(\alpha_c-\alpha+i\epsilon),\tag{8}$$

where

$$\alpha_c=1+\frac{1}{s'_{NN}}\left[\tilde m_N^2-\frac{m_s^2(1-x_1)+m_q^2x_1+(k_1-x_1p_1)^2}{x_1(1-x_1)}\right].\tag{9}$$

Here m_s^2 and $\tilde m_N^2\approx m_N^2$ are defined in Eqs. (A8) and (A11), and m_q represents the current quark mass of the knocked-out quark. Our further discussion is based on the use of the fact that the ^{3}He wave function strongly peaks at $\alpha=\frac{1}{2}$, which corresponds to the kinematic situation in which two constituent nucleons have equal share of the NN pair's light-cone momentum. Thus one expects that the integral in Eq. (7) is dominated by the value of the integrand at $\alpha=\alpha_c=\frac{1}{2}$. This allows us to perform α-integration in Eq. (7) through the pole of the denominator (8) at $\alpha=\alpha_c$ (i.e., keeping only the $-i\pi\delta(\alpha-\alpha_c)$ part of the relation $\frac{1}{\alpha_c-\alpha+i\epsilon}=-i\pi\delta(\alpha-\alpha_c)+P\frac{1}{\alpha_c-\alpha}$) and later replacing α_c by $\frac{1}{2}$. Using this relation to estimate the propagator of the struck quark at its on-mass shell value ($\alpha=\alpha_c$) allows us to represent $(\not p_{1i}-\not k_1+\not q)^{\text{on shell}}+m_q=\sum_\zeta u_\zeta(p_1-k_1+q)\bar u_\zeta(p_1-k_1+q)$. Then for the scattering amplitude of Eq. (7) one obtains

$$\langle\lambda_{1f},\lambda_{2f},\lambda_s|A_i|\lambda_\gamma,\lambda_A\rangle$$

$$=\sum_{(\eta_{1f},\eta_{2f}),(\eta_{1i},\eta_{2i}),(\lambda_{1i},\lambda_{2i}),\zeta}\int\Bigg\{\frac{\psi_N^{\dagger\lambda_{2f},\eta_{2f}}(p_{2f},x_2',k_{2\perp})}{1-x_2'}\bar u_{\eta_{2f}}$$

$$\times(p_{2f}-k_2)\left[-igT_c^F\gamma^\nu\right]$$

$$\times\frac{i\cdot u_\zeta(p_1-k_1+q)\bar u_\zeta(p_1-k_1+q)}{(1-x_1)s'}$$

$$\times\left[-iQ_ie\epsilon_\perp^{\lambda_\gamma}\gamma^\perp\right]u_{\eta_{1i}}(p_{1i}-k_1)\,\frac{\psi_N^{\lambda_{1i},\eta_{1i}}(p_{1i},x_1,k_{1\perp})}{(1-x_1)}\Bigg\}_1$$

$$\times\left\{\frac{\psi_N^{\dagger\lambda_{1f},\eta_{1f}}(p_{1f},x_1',k_{1\perp})}{1-x_1'}\,\bar u_{\eta_{1f}}(p_{1f}-k_1)\right.$$

$$\left.\times\left[-igT_c^F\gamma^\mu\right]u_{\eta_{2i}}(p_{2i}-k_2)\,\frac{\psi_N^{\lambda_{2i},\eta_{2i}}(p_{2i},x_2,k_{2\perp})}{(1-x_2)}\right\}_2$$

$$\times G^{\mu,\nu}(r)\frac{dx_1}{x_1}\frac{d^2k_{1\perp}}{2(2\pi)^3}\frac{dx_2}{x_2}\frac{d^2k_{2\perp}}{2(2\pi)^3}$$

$$\times\frac{\Psi_{^3\mathrm{He}}^{\lambda_A,\lambda_{1i},\lambda_{2i},\lambda_s}(\alpha_c,p_\perp,p_s)}{(1-\alpha_c)\alpha_c}\frac{d^2p_\perp}{4(2\pi)^2}-(p_{1f}\longleftrightarrow p_{2f}).\tag{10}$$

Next we evaluate the matrix element of the photon-quark interaction using on-mass shell spinors for the struck quark. Taking into account the fact that $(p_{1i}-k)_+\gg|k_\perp|,m_q$, for this matrix element we obtain

$$\bar u_\zeta(p_{1i}-k_1+q)[-iQ_ie\epsilon_\perp^{\lambda_\gamma}\gamma^\perp]u_{\eta_{1i}}(p_{1i}-k_1)$$
$$=ieQ_i2\sqrt{2E_2E_1}(\lambda_\gamma)\delta^{\lambda_\gamma\zeta}\delta^{\lambda_\gamma\eta_{1i}},\tag{11}$$

where $E_1=(1-\alpha)(1-x_1)\frac{\sqrt{s'_{NN}}}{2}$ and $E_2=(1-(1-\alpha)(1-x_1))\frac{\sqrt{s'_{NN}}}{2}$.

Further explicit calculations of Eq. (10) require the knowledge of quark wave functions of the nucleon. Also, one needs to sum over the multitude of the amplitudes representing different topologies of quark knock-out rescattering and recombinations into two final nucleon states.

We attempt to solve this problem by using the above observation that the ^{3}He wave function strongly peaks at

$\alpha = \frac{1}{2}$. We evaluate Eq. (10) setting everywhere $\alpha_c = \frac{1}{2}$. Such approximation significantly simplifies further derivations. As it follows from Eq. (9) the $\alpha_c = \frac{1}{2}$ condition restricts the values of x_1 of the recoil quark-gluon system to $x_1 \sim \frac{k_{1\perp}^2}{s'_{NN}}$, thereby ensuring that the quark-interchange happens for the valence quarks with $x_q = 1 - x_1 \sim 1$. The latter allows us to simplify Eq. (11) setting $E_1 = E_2 = \frac{\sqrt{s'_{NN}}}{4}$. Using these approximations and substituting Eq. (11) into Eq. (10) one obtains

$$
\begin{aligned}
&\langle \lambda_{1f}, \lambda_{2f}\lambda_s | A_i | \lambda_\gamma, \lambda_A \rangle \\
&= i[\lambda_\gamma] e \sum_{(\eta_{1f},\eta_{2f}),(\eta_{2i}),(\lambda_{1i},\lambda_{2i})} \int \frac{Q_i}{\sqrt{2s'}} \\
&\times \left[\left\{ \frac{\psi_N^{\dagger\lambda_{2f},\eta_{2f}}(p_{2f}, x'_2, k_{2\perp})}{1-x'_2} \bar{u}_{\eta_{2f}}(p_{2f} - k_2) \left[-igT_c^F \gamma^\nu \right] \right. \right. \\
&\times u_{\lambda_\gamma}(p_1 - k_1 + q) \left. \frac{\psi_N^{\lambda_{1i},\lambda_\gamma}(p_{1i}, x_1, k_{1\perp})}{(1-x_1)} \right\} \\
&\times \left\{ \frac{\psi_N^{\dagger\lambda_{1f},\eta_{1f}}(p_{1f}, x'_1, k_{1\perp})}{1-x'_1} \bar{u}_{\eta_{1f}}(p_{1f} - k_1) \right. \\
&\times \left[-igT_c^F \gamma^\mu \right] u_{\eta_{2i}}(p_{2i} - k_2) \left. \frac{\psi_N^{\lambda_{2i},\eta_{2i}}(p_{2i}, x_2, k_2)}{(1-x_2)} \right\} \\
&\times \left. G^{\mu,\nu}(r) \frac{dx_1}{x_1} \frac{d^2k_{1\perp}}{2(2\pi)^3} \frac{dx_2}{x_2} \frac{d^2k_{2\perp}}{2(2\pi)^3} \right]_{\rm QIM} \Psi_{^3{\rm He}}^{\lambda_A,\lambda_{1i},\lambda_{2i}} \\
&\times \left(\alpha = \frac{1}{2}, p_{2\perp} \right) \frac{d^2p_{2\perp}}{(2\pi)^2} - (p_{1f} \leftrightarrow p_{2f}). \qquad (12)
\end{aligned}
$$

Note that due to the δ factors in Eq. (11) the helicity of the knocked-out quark in Eq. (12) is equal to the helicity of incoming photon, that is, $\eta_{1i} = \lambda_\gamma$.

To proceed, we observe that the kernel $[\ldots]_{\rm QIM}$ representing the quark-interchange mechanism (QIM) of the rescattering in Eq. (12) can be identified with the quark-interchange contribution in the NN scattering amplitude (see Appendix B). Such identification can be done by observing that, in the chosen reference frame, $q_+ = 0$, and the quark wave function of the nucleon depends on the quark's light-cone momentum fraction and transverse momentum only, which are the same in both Eqs. (12) and (B4). For our derivation we also use the above-discussed observation that the $\alpha = \alpha_c = \frac{1}{2}$ condition ensures that the quark-interchange happens for the valence quarks with $x_q = 1 - x_1 \sim 1$. This justifies our next assumption, that valence quarks carry the helicity of their parent nucleon (i.e., $\eta_{1i} = \lambda_i$). The last assumption allows us to perform the summation of Eq. (12) over the helicities of the exchanged quarks ($\eta_{2i}, \eta_{1f}, \eta_{2f}$) and to use Eq. (B4) to express the QIM part in Eq. (12) through the corresponding QIM amplitude of NN scattering. Summing for all possible topologies of quark-interchange diagrams we arrive at

$$
\begin{aligned}
&\langle \lambda_{1f}, \lambda_{2f}, \lambda_s | A | \lambda_\gamma, \lambda_A \rangle \\
&= ie[\lambda_\gamma] \left\{ \sum_{i\in N_1} \sum_{\lambda_{2i}} \int \frac{Q_i^{N_1}}{\sqrt{2s'}} \langle \lambda_{2f}; \lambda_{1f} | T_{NN,i}^{\rm QIM}(s, l^2) \right. \\
&\times |\lambda_\gamma; \lambda_{2i}\rangle \Psi_{^3{\rm He}}^{\lambda_A}(p_1, \lambda_\gamma; p_2, \lambda_{2i}, p_s, \lambda_s) \frac{d^2p_\perp}{(2\pi)^2} \\
&+ \sum_{i\in N_2} \sum_{\lambda_{1i}} \int \frac{Q_i^{N_2}}{\sqrt{2s'}} \langle \lambda_{2f}; \lambda_{1f} | T_{NN,i}^{\rm QIM}(s, l^2) | \lambda_{1i}; \lambda_\gamma \rangle \\
&\times \left. \Psi_{^3{\rm He}}^{\lambda_A}(p_1, \lambda_{1i}; p_2, \lambda_\gamma, p_s, \lambda_s) \frac{d^2p_\perp}{(2\pi)^2} \right\}, \qquad (13)
\end{aligned}
$$

where nucleon momenta p_1 and p_2 have half of their c.m. momentum fractions and $p_\perp$ is their relative transverse momentum with respect to the direction of the photon momentum [see Eq. (20)]. Here, for example, $Q_i^N \cdot \langle \lambda_{2f}; \lambda_{1f} | T_{NN,i}^{\rm QIM}(s, l^2) | \lambda_1; \lambda_2 \rangle$ represents the quark-interchange amplitude of NN interaction weighted with the charge of those interchanging quarks Q_i^N that are struck from a nucleon N by the incoming photon. The sum ($\sum_{i\in N}$) can be performed within the quark-interchange model of NN interaction, which allows us to represent the NN scattering amplitude as follows [29]:

$$
\langle a'b' | T_{NN}^{\rm QIM} | ab \rangle = \frac{1}{2} \langle a'b' | \sum_{i\in a, j\in b} [I_i I_j + \vec{\tau}_i \vec{\tau}_j] F_{i,j}(s,t) | ab \rangle, \qquad (14)
$$

where I_i and τ_i are the identity and Pauli matrices defined in the SU(2) flavor (isospin) space of the interchanged quarks. The kernel $F_{i,j}(s,t)$ describes an interchange of i and j quarks.[2]

Using Eq. (14) one can calculate the quark-charge weighted QIM amplitude, $Q_i \cdot \langle a'b' | T_{NN,i}^{\rm QIM} | ab \rangle$, as follows:

$$
\begin{aligned}
&\sum_{i\in N} Q_i^N \langle a'b' | T_{NN,i}^{\rm QIM} | ab \rangle \\
&= \frac{1}{2} \langle a'b' | \sum_{i\in a, j\in b} [I_i I_j + \vec{\tau}_i \vec{\tau}_j] (Q_i) F_{i,j}(s,t) | ab \rangle \\
&= Q_F^N \cdot \langle a'b' | T_{NN}^{\rm QIM} | ab \rangle, \qquad (15)
\end{aligned}
$$

where Q_F^N are the charge factors that are explicitly calculated using the method described in Appendix C. These factors can be expressed through the combinations of valence quark charges Q_i of nucleon N and the number of quark interchanges for each flavor of quark, N_{Q_i}, necessary to produce a given helicity NN amplitude, as follows,

$$
Q_F^N = \frac{N_{uu}(Q_u) + N_{dd}(Q_d) + N_{ud}(Q_u + Q_d)}{N_{uu} + N_{dd} + N_{ud}}. \qquad (16)
$$

Next we discuss the light-cone wave function of ^{3}He that enters in Eq. (13). The important result that allows us to evaluate the wave function is the observation that two nucleons that interact with the photon share equally the NN pair's c.m. momentum (p_{NN}), i.e., $\alpha = \frac{1}{2}$. If we constrain the

[2]The additional assumption of helicity conservation allows us to express the kernel in the form [29] $F_{i,j}(s,t) = \frac{1}{2}[I_i I_j + \vec{\sigma}_i \vec{\sigma}_j] \tilde{F}_{i,j}(s,t)$, where I_i and σ_i operate in the SU(2) helicity (H-spin) space of exchanged (i,j) quarks [29]. However, for our discussion the assumption of helicity conservation is not required.

third nucleon's light-cone momentum fraction $\alpha_s = \frac{3\cdot p_{s+}}{p_{^3\mathrm{He}+}} = \frac{3(E_s+p_s^z)}{E_{^3\mathrm{He}}+p_s^z+p_{NN}^z} \approx 1$ and transverse momentum $p_{s\perp} \ll m_N$, then the momenta of all the nucleons in the nucleus are nonrelativistic. In this case one can use the calculation of triangle diagrams, which provides the normalization of nuclear wave functions based on baryonic number conservation to relate LC and nonrelativistic nuclear wave functions, as follows [30,31]

$$\Psi_{^3\mathrm{He}}(\alpha,\, p_\perp, \alpha_s,\, p_{s,\perp}) = \sqrt{2}(2\pi)^3 m_N \Psi_{^3\mathrm{He,NR}}(\alpha,\, p_\perp, \alpha_s,\, p_{s,\perp}), \tag{17}$$

where for $\Psi_{^3\mathrm{He,NR}}$ we can use known nonrelativistic ^{3}He wave functions (see, e.g., Ref. [32]).

Substituting Eqs. (15) and (17) into Eq. (13) for the two-nucleon photodisintegration amplitude we obtain

$$\begin{aligned}
&\langle \lambda_{1f}, \lambda_{2f}, \lambda_s | M | \lambda_\gamma, \lambda_A \rangle \\
&= \frac{i[\lambda_\gamma] e\sqrt{2}(2\pi)^3}{\sqrt{2S'_{NN}}} \times \Bigg\{ Q_F^{N_1} \sum_{\lambda_{2i}} \int \langle \lambda_{2f}; \lambda_{1f} | \\
&\quad \times T_{NN}^{\mathrm{QIM}}(s_{NN}, t_N) | \lambda_\gamma; \lambda_{2i} \rangle \Psi^{\lambda_A}_{^3\mathrm{He,NR}} \\
&\quad \times (\vec{p}_1, \lambda_\gamma; \vec{p}_2, \lambda_{2i}; \vec{p}_s, \lambda_s) m_N \frac{d^2 p_\perp}{(2\pi)^2} \\
&\quad + Q_F^{N_2} \sum_{\lambda_{1i}} \int \langle \lambda_{2f}; \lambda_{1f} | T_{NN}^{\mathrm{QIM}}(s_{NN}, t_N) | \lambda_{1i}; \lambda_\lambda \rangle \\
&\quad \times \Psi^{\lambda_A}_{^3\mathrm{He,NR}}(\vec{p}_1, \lambda_{1i}; \vec{p}_2, \lambda_\gamma; \vec{p}_s, \lambda_s) m_N \frac{d^2 p_\perp}{(2\pi)^2} \Bigg\},
\end{aligned} \tag{18}$$

where in the Lab frame of the ^{3}He nucleus, defining the z direction along the direction of q_{Lab} one obtains

$$\begin{aligned}
\alpha &= \frac{E_2 - p_{2z}}{M_A - E_s - p_{sz}}; \quad p_\perp = \frac{p_{1\perp} - p_{2\perp}}{2}, \\
\alpha_s &= \frac{E_s + p_{sz}}{M_A/A}; \quad \vec{p}_1 + \vec{p}_2 = -\vec{p}_s,
\end{aligned} \tag{19}$$

with all the momenta defined in the Lab frame.

Equation (18) allows us to calculate the unpolarized differential cross section of two nucleon breakup in the form

$$\frac{d\sigma}{dt d^3 p_s/(2E_s(2\pi)^3)} = \frac{|\bar{\mathcal{M}}|^2}{16\pi\big(s - M_A^2\big)\big(s_{NN} - M_{NN}^2\big)}, \tag{20}$$

where $s = (k_\gamma + p_A)^2$ and

$$|\bar{M}|^2 = \frac{1}{2}\cdot\frac{1}{2} \sum_{\lambda_{1f},\lambda_{2f},\lambda_s,\lambda_\gamma,\lambda_A} |\langle \lambda_{1f}, \lambda_{2f}, \lambda_s | M | \lambda_\gamma, \lambda_A \rangle|^2. \tag{21}$$

As follows from Eq. (18) the knowledge of quark-interchange helicity amplitudes of NN elastic scattering will allow us to calculate the differential cross section of hard NN breakup reaction without introducing any adjustable parameter.

Because the assumption of $\alpha_c = \frac{1}{2}$ plays a major role in the above derivations we attempt now to estimate the theoretical error introduced by this approximation. This approximation by its nature is a "peaking" approximation that is used in loop calculations involving Feynman diagrams (one such example is the calculation of radiative effects in electroproduction processes; see, e.g., Ref. [33]). One way to estimate the accuracy of the approximation is to identify the main dependence of the integrand in Eq. (10) on α_c, which can be evaluated exactly, and compare with its evaluation at $\alpha_c = \frac{1}{2}$. Using Eq. (11) as well as Eq. (9) that allows us to relate $\frac{dx_1}{x_1}$ to $\frac{d\alpha_c}{\alpha_c}$, and assuming that the quark wave functions of nucleons at $\alpha_c \sim \frac{1}{2}$ are less sensitive to α_c, one arrives at

$$R(p_s) = \frac{4\Psi^{\lambda_A,\lambda_{1i},\lambda_{2i},\lambda_s}_{^3\mathrm{He}}\big(\alpha_c = \frac{1}{2},\, p_\perp,\, p_s\big)}{\int \frac{d\alpha_c}{\alpha_c} \frac{\Psi^{\lambda_A,\lambda_{1i},\lambda_{2i},\lambda_s}_{^3\mathrm{He}}(\alpha_c, p_\perp, p_s)}{\sqrt{(1-\alpha_c)\alpha_c}}}. \tag{22}$$

This ratio depends on the kinematics of the spectator nucleon, and for the case of $p_s \leqslant 100$ MeV/c, $R(p_s) \approx 1.1$, which corresponds to $\sim$20% of uncertainty in the cross section of the reaction calculated with the $\alpha_c = \frac{1}{2}$ approximation. The uncertainty increases with an increase of the momentum of the spectator nucleon. This can be understood qualitatively because, for large center of mass momenta of the NN pair, the $\alpha = \frac{1}{2}$ peak of the nuclear wave function is less pronounced.

C. Quark-interchange and hard NN elastic scattering amplitudes

The possibility of using NN elastic scattering data to calculate the cross section in Eqs. (20) and (21) is based on the assumption that the quark-interchange mechanism provides the bulk of the NN elastic scattering strength at high energies and large c.m. angles. This is a rather well-justified assumption. Experiments on exclusive large $-t$ two-body reactions [34] demonstrated clearly the dominance of the quark-interchange mechanism for the scattering of hadrons that share common quark flavors. The analysis of these experiments indicate that contributions from competing mechanisms such as pure gluon exchange or quark-antiquark annihilation are on the level of a few percent. This justifies our next approximation, to substitute quark-interchange NN amplitudes in Eq. (18) with actual NN helicity amplitudes as follows:

$$\begin{aligned}
\langle +,+ | T_{NN}^{\mathrm{QIM}} | +,+ \rangle &= \phi_1 \\
\langle +,+ | T_{NN}^{\mathrm{QIM}} | +,- \rangle &= \phi_5 \\
\langle +,+ | T_{NN}^{\mathrm{QIM}} | -,- \rangle &= \phi_2 \\
\langle +,- | T_{NN}^{\mathrm{QIM}} | +,- \rangle &= \phi_3 \\
\langle +- | T_{NN}^{\mathrm{QIM}} | -+ \rangle &= -\phi_4.
\end{aligned} \tag{23}$$

All other helicity combinations can be related to the above amplitudes through the parity and time-reversal symmetry. The minus sign in the last equation above is due to the Jackob-Wick phase factor (see, e.g., Ref. [35]), according to which one gains a phase factor of (-1) if two quarks that scatter by $\pi - \theta$ angle in c.m. have opposite helicities [36]. Note that ϕ_i's are normalized in such a way that the cross section for

NN scattering is defined as

$$\frac{d\sigma^{NN\to NN}}{dt} = \frac{1}{16\pi}\frac{1}{s(s-4m_N^2)}\frac{1}{2}(|\phi_1|^2 + |\phi_2|^2 + |\phi_3|^2 + |\phi_4|^2 + 4|\phi_5|^2). \quad (24)$$

Because in the hard breakup regime the momentum transfer $-t_N \gg m_N^2$, one can factorize the helicity NN amplitudes from Eq. (18) at s_{NN} and t_N values defined as follows:

$$s_{NN} = (q + p_{NN})^2 = (p_{f1} + p_{f2})^2,$$
$$t_N = (p_{f2} - p_{NN}/2)^2 = \frac{t_{NN}}{2} + \frac{m_N^2}{2} - \frac{M_{NN}^2}{4}. \quad (25)$$

Using this factorization in Eq. (18) for the spin averaged square of the breakup amplitude one obtains

$$|\bar{\mathcal{M}}|^2 = \frac{(e^2 2(2\pi)^6}{2s'_{NN}}\frac{1}{2}\{2Q_F^2|\phi_5|^2 S_0 + Q_F^2(|\phi_1|^2 + |\phi_2|^2)S_{12} + [(Q_F^{N_1}\phi_3 + Q_F^{N_2}\phi_4)^2 + (Q_F^{N_1}\phi_4 + Q_F^{N_2}\phi_3)^2)]S_{34}\}, \quad (26)$$

where $Q_F = Q_F^{N_1} + Q_F^{N_2}$ and S_{12}, S_{34}, and S_0 are partially integrated nuclear spectral functions:

$$S_{12}(t_1, t_2, \alpha, \vec{p}_s) = N_{NN}\sum_{\lambda_1=\lambda_2=-\frac{1}{2}}^{\frac{1}{2}}\sum_{\lambda_3=-\frac{1}{2}}^{\frac{1}{2}}\left|\int \Psi^{\frac{1}{2}}_{^3\mathrm{He,NR}} \times(\vec{p}_1, \lambda_1, t_1; \vec{p}_2, \lambda_2, t_2; \vec{p}_s, \lambda_3) m_N \frac{d^2p_\perp}{(2\pi)^2}\right|^2, \quad (27)$$

$$S_{34}(t_1, t_2, \alpha, \vec{p}_s) = N_{NN}\sum_{\lambda_1=-\lambda_2=-\frac{1}{2}}^{\frac{1}{2}}\sum_{\lambda_3=-\frac{1}{2}}^{\frac{1}{2}}\left|\int \Psi^{\frac{1}{2}}_{^3\mathrm{He,NR}} \times(\vec{p}_1, \lambda_1, t_1; \vec{p}_2, \lambda_2, t_2; \vec{p}_s, \lambda_3) m_N \frac{d^2p_\perp}{(2\pi)^2}\right|^2 \quad (28)$$

and

$$S_0 = S_{12} + S_{34}. \quad (29)$$

In the above equations t_1 and t_2 are the isospin projections of nucleons in ^{3}He. The wave function is normalized to $\frac{2}{3}$ for proton and $\frac{1}{3}$ for neutron. The normalization constants, N_{NN}, renormalize the wave function to one pp and two np effective pairs in the wave function with $N_{pp} = \frac{1}{2}$ and $N_{pn} = 4$.

Equations (20) and (26) together with Eqs. (24), (27), and (28) allow us to calculate the differential cross section of both pp and pn breakup reactions off the ^{3}He target. Notice that, on the qualitative level, as it follows from Eqs. (20) and (26) in the limit of $s \gg M_{^3\mathrm{He}}^2$ and $s_{NN} \gg m_N^2$, the HRM predicts an s^{-11} invariant energy dependence of the differential cross section provided that the NN cross section scales as s^{-10}. However, the numerical calculations of Eq. (26) require a knowledge of the NN helicity amplitudes at high energy and momentum transfers. Our strategy is to use Eq. (24) to express NN breakup reactions directly through the differential cross section of pn and pp elastic scatterings rather than to use helicity amplitudes explicitly.

III. HARD BREAKUP OF PROTON AND NEUTRON FROM ^{3}He

We consider now the reaction

$$\gamma + {}^3\mathrm{He} \to (pn) + p, \quad (30)$$

in which one proton is very energetic and produced at large c.m. angles with the neutron, while the second proton emerges with low momentum $\lesssim 100$ MeV/c. In this case the hard rescattering happens in the pn channel. Using the $\phi_3 \approx \phi_4$ relation for hard pn scattering amplitude (see, e.g., Refs. [29,35,37]) for breakup amplitude of Eq. (26) one obtains

$$|\bar{\mathcal{M}}|^2 = \frac{(Q_F^{pn}e)^2 2(2\pi)^6}{2s'_{NN}}\frac{1}{2}\{2|\phi_5|^2 S_0 + (|\phi_1|^2 + |\phi_2|^2)S_{12} + (|\phi_3|^2 + |\phi_4|^2)S_{34}\}, \quad (31)$$

where $Q_F^{(pn)} = Q_F^p + Q_F^n$ can be calculated using Eqs. (15) and (16). Based on SU(6) flavor-spin symmetry of nucleon wave functions, for the helicity amplitudes of Eq. (24) using the method described in Appendix C one obtains

$$Q_F^{pn} = \tfrac{1}{3}. \quad (32)$$

We can further simplify Eq. (31) noticing that for the pn pair in ^{3}He one has $S_{12} \approx S_{34} \approx \frac{S_0}{2}$. This is due to the fact that in the dominant S state two protons have opposite spins and therefore the probability of finding one proton with a helicity opposite to that of the neutron is equal to the other proton having the same helicity as the neutron's. Using this relation and Eq. (24) for the pn breakup reaction one obtains

$$|\bar{M}|^2 = \frac{(eQ_{F,pn})^2(2\pi)^6}{s'_{NN}} 16\pi s_{NN}(s_{NN} - 4m_N^2) \times \frac{d\sigma^{pn\to pn}(s_{NN}, t_N)}{dt_N}\frac{S_0^{pn}}{2}. \quad (33)$$

Inserting it in Eq. (20) for the differential cross section one obtains

$$\frac{d\sigma^{\gamma\,^3\mathrm{He}\to(pn)p}}{dt\,\frac{d^3p_s}{E_s}} = \alpha Q_{F,pn}^2 16\pi^4 \frac{S_0^{pn}(\alpha = \frac{1}{2}, \vec{p}_s)}{2} \times \frac{s_{NN}(s_{NN} - 4m^2)}{(s_{NN} - p_{NN}^2)_{NN}^2(s - M_{^3\mathrm{He}}^2)} \times \frac{d\sigma^{pn\to pn}(s_{NN}, t_N)}{dt_N}, \quad (34)$$

where $\alpha = \frac{1}{137}$ and $\frac{d\sigma^{pn\to pn}}{dt_N}$ is the differential cross section of hard pn scattering evaluated at values of s_{NN} and t_N defined in Eq. (25). The spectral function S_0^{pn} is defined in Eq. (29) and corresponds to

$$S_0^{pn}(\alpha, \vec{p}_s) = 4\sum_{\lambda_1,\lambda_2,\lambda_3=-\frac{1}{2}}^{\frac{1}{2}}\left|\int \Psi^{\frac{1}{2}}_{^3\mathrm{He,NR}} \times\left(\vec{p}_1, \lambda_1, \frac{1}{2}; \vec{p}_2, \lambda_2 - \frac{1}{2}; \vec{p}_s, \lambda_3\right) m_N \frac{d^2p_\perp}{(2\pi)^2}\right|^2. \quad (35)$$

IV. HARD BREAKUP OF TWO PROTONS FROM ^{3}He

We now consider the reaction

$$\gamma + {}^3\mathrm{He} \to (pp) + n, \tag{36}$$

in which two protons are produced at large c.m. angles while the neutron emerges as a spectator with small momentum ($p_s \leqslant 100$ MeV/c).

We observe now that the relation between S_{12} and S_{34} is very different from that of the pn case. Due to the fact that two protons cannot have the same helicity in the S state one has $S_{12} \ll S_{34}$. The estimates of the spectral functions based on the realistic ^{3}He wave function [32] gives $\frac{S_{12}}{S_{34}} \sim 10^{-4}$. Therefore one can neglect the S_{12} term in Eq. (26). The next observation is that for pp scattering the helicity amplitudes ϕ_3 and ϕ_4 have opposite signs due to the Pauli principle (see, e.g., Refs. [35,36]). Using the above observations and neglecting the helicity-nonconserving amplitude ϕ_5 for the pp breakup amplitude we obtain

$$|\bar{\mathcal{M}}|^2 = \frac{(e^2 2(2\pi)^6}{2s'_{NN}} \frac{1}{2}\left\{2\left(Q_F^p|\phi_3| - Q_F^p|\phi_4|\right)^2 S_{34}\right\}. \tag{37}$$

The charge factor Q_F^p depends on the helicity amplitude it couples; therefore one estimates it for the combination of $(Q_F^p|\phi_3| - Q_F^p|\phi_4|)$. Using SU(6) symmetry for the distribution of given helicity-flavor valence quarks in the proton and through the approach described in Appendix C we obtain

$$\left(Q_F^p|\phi_3| - Q_F^p|\phi_4|\right) = Q_F^{pp}(|\phi_3| - |\phi_4|), \tag{38}$$

with

$$Q_F^{pp} = \tfrac{5}{3}. \tag{39}$$

It is worth noticing that due to explicit consideration of quark degrees of freedom the effective charge involved in the breakup is larger for the case of two protons than for proton and neutron [see Eq. (32)]. This is characteristic of the HRM model in which a photon couples to a quark and more charges are exchanged in the pp case than in the pn case. This is rather opposite to the scattering picture considered based on hadronic degrees of freedom in which case the photon will couple to an exchanged meson and pp contribution will be significantly suppressed because no charged mesons can be exchanged within the pp pair.

To be able to estimate the cross section of the pp breakup reaction through the elastic pp scattering cross section we introduce a parameter

$$C^2 = \frac{\phi_3^2}{\phi_1^2} \approx \frac{\phi_4^2}{\phi_1^2}, \tag{40}$$

which allows to express the differential cross section of the reaction (36) in the following form:

$$\frac{d\sigma^{\gamma\,{}^3\mathrm{He}\to(pp)n}}{dt\,\frac{d^3p_s}{E_s}} = \alpha Q_{F,pp}^2 16\pi^4 S_{34}^{pp}\left(\alpha = \frac{1}{2}, \vec{p}_s\right)\frac{2\beta^2}{1+2C^2} \times \frac{s_{NN}\left(s_{NN} - 4m_N^2\right)}{\left(s_{NN} - p_{NN}^2\right)^2\left(s - M_{^3\mathrm{He}}^2\right)} \times \frac{d\sigma^{pp\to pp}(s_{NN}, t_N)}{dt}, \tag{41}$$

where we also introduced a factor β,

$$\beta = \frac{|\phi_3| - |\phi_4|}{|\phi_1|}, \tag{42}$$

which accounts for the suppression due to the cancellation between ϕ_3 and ϕ_4 helicity amplitudes of elastic pp scattering.[3] The spectral function S_{34}^{pp} in Eq. (41) is expressed through the ^{3}He wave function according to Eq. (28) as follows:

$$S_{34}^{pp}(\alpha, \vec{p}_s) = \frac{1}{2}\sum_{\lambda_1=-\lambda_2=-\frac{1}{2}}^{\frac{1}{2}}\sum_{\lambda_3=-\frac{1}{2}}^{\frac{1}{2}}\left|\int \Psi_{^3\mathrm{He,NR}}^{\frac{1}{2}} \times \left(\vec{p}_1, \lambda_1, \frac{1}{2}; \vec{p}_2, \lambda_2, \frac{1}{2}; \vec{p}_s, \lambda_3\right) m_N \frac{d^2 p_{2,\perp}}{(2\pi)^2}\right|^2. \tag{43}$$

V. TWO- AND THREE-BODY PROCESSES IN NN BREAKUP REACTIONS

For a two-body hard NN breakup mechanism to be observed it must dominate the three-body/two-step processes. This is especially important for pp breakup processes (36), because according to Eqs. (41) and (42) the two-body contribution is suppressed because of a cancellation between ϕ_3 and ϕ_4 helicity amplitudes.

At low to intermediate range energies ($E_\gamma \sim 200$ MeV) it is rather well established that the pp breakup reaction proceeds overwhelmingly through a two-step (three-body) process [38–43] in which the initial breakup of the pn pair (dominated by $\pi^\pm$ exchange) is followed by a charge-interchange final state interaction of the neutron with the spectator proton. Other two-step processes include the excitation of intermediate Δ isobars in the pn system with the subsequent rescattering off the spectator neutron, which produces two final protons.

The dominance of three-body processes at low energies is related mainly to the fact that the two-body pp breakup is negligible because of the impossibility of charged-pion exchanges between two protons that absorb an incoming photon.

At high energy kinematics within the HRM the interaction between protons is carried out by exchanged quarks because of which the relative strength of pp breakup is larger.

To estimate the strength of three-body processes at high energy kinematics, one needs to calculate the contribution of diagrams similar to Fig. 2. Because the charge-exchange rescattering at the final stage of the process in Fig. 2 takes place at proton momenta $p'_f > m_N$, one can apply an eikonal approximation [44,45] to estimate its contribution.

For $E_\gamma \geqslant 2$ GeV assuming that the HRM is valid for the first (pn breakup) stage of the reaction, for the amplitude of three-body/two-step process within the eikonal approximation

[3] This cancellation was overlooked in our early estimate of the cross section of pp photodisintegration from ^{3}He target (see, e.g., Ref. [27]).

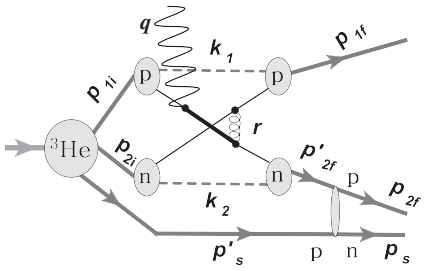

FIG. 2. Diagram corresponding to three-body processes in which the hard breakup of the pn pair is followed by a soft charge-exchange rescattering of the neutron off the spectator proton.

[44,45] one obtains

$$M_{3\text{body}} \approx \frac{eQ_{F,pn}(2\pi)^3}{2\sqrt{2s'_{NN}}} T^{\text{hard}}_{pn\to pn}(t_N) \int \Psi^{\lambda_A}_{^3\text{He,NR}}(\vec{p}_1, t_1; \vec{p}_2, t_2; \times \vec{p}_s - \vec{k}_\perp) m_N \frac{T^{\text{chex}}_{pn\to np}(k_\perp)}{s_{NN}} \frac{d^2p_\perp}{(2\pi)^2} \frac{d^2k_\perp}{(2\pi)^2}, \quad (44)$$

where we suppressed helicity indices for simplicity and choose the isospin projections, $t_1 = -t_2 = \frac{1}{2}$, corresponding to the initial pn pair that interacts with the photon. Here $T^{\text{hard}}_{pn\to pn}(t_N)$ is the hard elastic pn scattering amplitude and $T^{\text{chex}}_{pn\to np}$ represents the amplitude of the soft charge-exchange pn scattering. Because of the pion-exchange nature of the latter it is rather well established that this amplitude is real and can be represented as $\sim\sqrt{s}Ae^{\frac{B}{2}t}$, where A and B are approximately constants [46].

Two main observations follow from Eq. (44) and the above-mentioned property of the charge-exchange amplitude: First, three-body and two-body amplitudes [see, e.g., Eq. (18)] will not interfere, because one is real and the other is imaginary. The fact that these two amplitudes differ by order of i follows from the general structure of rescattering amplitudes (see, e.g., Ref. [45]). Equation (18) corresponds to a single rescattering amplitude, while Eq. (44) corresponds to a double rescattering amplitude. Second, because of the energy dependence of the charge-exchange scattering amplitude at small angles, the three-body contribution will scale like s^{-12} as compared to the two-body breakup contribution.

Using Eq. (44) one can estimate the magnitude of the contribution of three-body processes in the pp breakup cross section as follows:

$$\frac{d\sigma^{\gamma^3\text{He}\to(pp)n}_{\text{three-body}}}{dt\,\frac{d^3p_s}{E_s}} \approx \frac{d\sigma^{\gamma^3\text{He}\to(pn)p}_{\text{two-body}}}{dt\,\frac{d^3p_s}{E_s}} \frac{S^{pnp}(p_s)}{S_0^{pn}(p_s)}, \quad (45)$$

where $S_0^{pn}(p_s)$ is defined in Eq. (35) and for $S^{pnp}(p_s)$ based on Eq. (44) one obtains

$$S^{pnp}(p_s) = \frac{N_{pn}}{16s_{NN}^2} \left| \int \Psi^{\lambda_A}_{^3\text{He,NR}}(\vec{p}_1, \vec{p}_2, \vec{p}_s - \vec{k}_\perp) m_N \times T^{\text{chex}}_{pn\to np}(k_\perp) \frac{d^2p_\perp}{(2\pi)^2} \frac{d^2k_\perp}{(2\pi)^2} \right|^2. \quad (46)$$

Here both spectral functions are defined at $\alpha = \frac{1}{2}$.

Using Eqs. (45) and (46) and the parametrization of $T^{\text{chex}}_{pn\to np}$ from Ref. [46] one can estimate the relative contribution of three-body processes numerically. Note that this contribution is maximal at $\alpha_s = 1$ and increases with an increase of the momentum of p_s. However because of the charge-exchange nature of the second rescattering, this contribution decreases linearly with an increase of s.[4]

VI. NUMERICAL ESTIMATES

For numerical estimates we consider the center of mass reference frame of the γ-NN system, for which according to Eq. (6) one obtains

$$t_{N,N} = -\frac{(s_{NN} - M_{NN}^2)}{2\sqrt{s_{NN}}} \times \left(\sqrt{s_{NN}} - \sqrt{s_{NN} - 4m_N^2}\cos(\theta_{\text{c.m.}})\right) + m_N^2, \quad (47)$$

where $M_{NN}^2 = p_{NN}^\mu p_{NN,\mu}$ and $p_{NN}^\mu = p_{^3\text{He}}^\mu - p_s^\mu$. Using the above equation we obtain for t_N [Eq. (25)], which defines the effective momentum transfer in the NN scattering amplitude, the following relation:

$$t_N = -\frac{(s_{NN} - M_{NN}^2)}{4\sqrt{s_{NN}}} \left(\sqrt{s_{NN}} - \sqrt{s_{NN} - 4m_N^2}\cos(\theta_{\text{c.m.}})\right) + m_N^2 - \frac{M_{NN}^2}{4}. \quad (48)$$

One can also calculate the effective c.m. angle that enters in the NN scattering amplitude as follows:

$$\cos\left(\theta^N_{\text{c.m.}}\right) = 1 - \frac{(s_{NN} - M_{NN}^2)}{2(s_{NN} - 4m_N^2)} \frac{\left(\sqrt{s_{NN}} - \sqrt{s_{NN} - 4m_N^2}\cos(\theta_{\text{c.m.}})\right)}{\sqrt{s_{NN}}} + \frac{4m_N^2 - M_{NN}^2}{2(s_{NN} - 4m_N^2)}. \quad (49)$$

The above equations define the kinematics of hard NN rescattering.

A. Energy dependence and the magnitude of the cross sections

We are interested in energy dependences of the hard breakup reactions of Eqs. (30) and (36) at fixed and large angle production of two fast nucleons in the γ-NN center of mass reference frame. Particularly interesting is the case of $\theta_{\text{c.m.}} = 90^\circ$ for which, as it follows from Eq. (49), $\cos(\theta^N_{\text{c.m.}}) = 0.5$. This means that the cross sections of hard breakup reactions at these kinematics will be defined by the NN elastic scattering at $\theta^N_{\text{c.m.}} = 60^\circ$. In Fig. 3 the E_γ and s dependencies of the s_{NN}^{11} weighted differential cross sections are presented for the cases of the pp and pn breakup reactions. In the calculation we integrated over the spectator nucleon's momentum in the range of (0–100) MeV/c and over the whole range of its solid angle. Also for the parameter C in Eq. (40) we

[4]Notice that for the case of diagonal $pn \to pn$ rescattering $T_{pn\to np}(k_\perp) = s\sigma_{\text{tot}}e^{\frac{B}{2}t}$ and as a result the probability of the rescattering is energy independent.

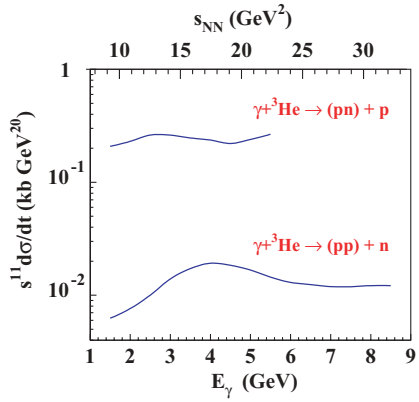

FIG. 3. (Color online) Energy dependence of s^{11} weighted differential cross sections at 90° c.m. angle scattering in the γ-NN system. In these calculations one integrated over the spectator nucleon momenta in the range of 0–100 MeV/c.

used $C = \frac{1}{2}$, consistent with an estimate obtained within the quark-interchange model of pp scattering (see, e.g., Refs. [29,35]). The estimation of the factor β, which takes into account the cancellation between ϕ_3 and ϕ_4 helicity amplitudes in Eq. (41), requires the knowledge of the angular dependence for helicity amplitudes. For this we used the helicity amplitudes calculated within the quark-interchange model [29,35] with phenomenological angular dependencies estimated using $F(\theta_{\text{c.m.}}) = \frac{1}{\sin^2(\theta_{\text{c.m.}})(1-\cos(\theta_{\text{c.m.}}))^2}$ (see, e.g., Refs. [29,37]) which describes reasonably well the data at hard scattering kinematics.

Several features of HRM calculations are worth discussing in Fig. 3: First, the breakup cross sections in average scale like s_{NN}^{-11}. Note that the absolute (nonscaled) values of the cross sections drop by five orders of magnitude in the 2–8 GeV photon energy range. Next, the shapes of the s^{11} weighted differential cross sections reflect the shapes of the s^{10} weighted differential cross sections of pp and pn scattering at $\theta_{\text{c.m.}} = 60°$ [see Figs. (4) and (5)]. It is worth noting that as follows from Figs. (4) and (5) the fits used in the calculation of pp and pn breakup reactions contain uncertainties on the level of 10% for pp breakup (for $s_{NN} \geqslant 24$ GeV^2) and up to 30% for pn breakup reactions. Based on this, one can conclude that the calculated shape of the energy dependence of the pn breakup reaction in Fig. (3) does not have much predictive power. However, for the pp breakup the calculated shape, for up to $s_{NN} \leqslant 24$ GeV^2, is not obscured by the uncertainty of the pp data and can be considered as a prediction of the HRM. It is worth mentioning that considered features of the HRM are insensitive to the choice of the above-discussed parameters of C and β, because they only define the absolute magnitude of the pp breakup cross section.

The next feature of the calculations in Fig. 3 is the magnitude of the pn and pp breakup cross sections. The pn breakup cross section [Eq. (34)] does not contain any free parameter and, similar to the HRM prediction for the breakup of the deuteron [22], it is expressed through the rather well-defined quantities. For the estimate of pp breakup, however, one needs to know the relative strength of the ϕ_3 and ϕ_4 amplitudes as compared to ϕ_1 as well as the extent

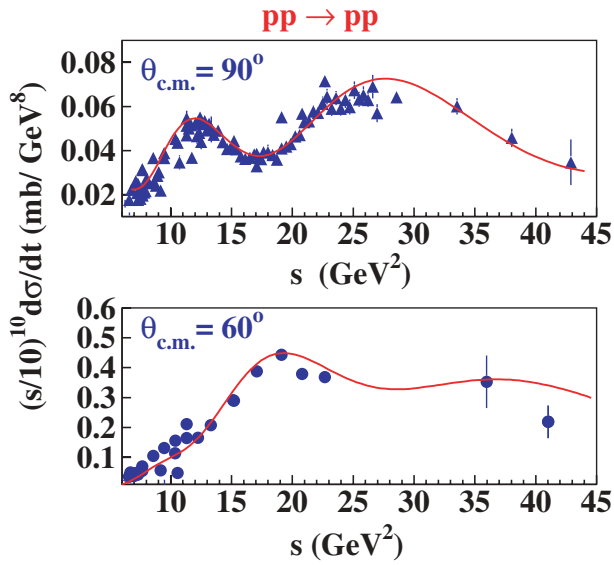

FIG. 4. (Color online) Invariant energy dependence of s^{10} weighted differential cross sections of elastic pp scattering at $\theta_{\text{c.m.}} = 90°$ and $\theta_{\text{c.m.}} = 60°$. Curves are the fits [47] of the available world data [48].

of their cancellation at kinematics of s_{NN} and t_N defined in Eqs. (25) and (48). Our calculation, based on phenomenologically justified estimates of factors C and β in Eq. (41) results in the pp breakup cross section which is about ten times smaller than the cross section for the pn breakup. This magnitude indicates, however, an increase of pp breakup cross section relative to the pn breakup cross section as compared to the results from the low energy breakup reactions. As it was mentioned in Sec. V at low energies (∼200 MeV) the cross section of pp photodisintegration from ^{3}He is significantly

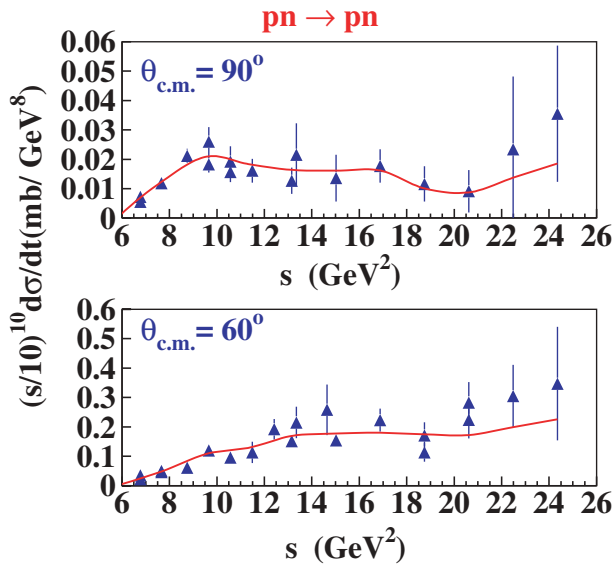

FIG. 5. (Color online) Invariant energy dependence of s^{10} weighted differential cross sections of elastic pn scattering at $\theta_{\text{c.m.}} = 90°$ and $\theta_{\text{c.m.}} = 60°$. Curves are the fits [47] of the available world data [48].

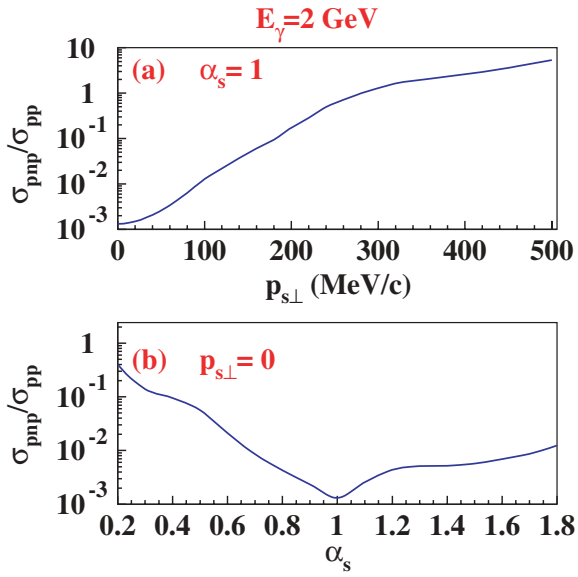

FIG. 6. (Color online) Dependence of the ratio of the cross section of three-body/two-step process discussed in Sec. V to the cross section of the two-body pp breakup at $E\gamma = 2$ GeV on (a) transverse momentum of the spectator neutron p_{st} at $\alpha_s = 1$ and on (b) α_s at $p_{st} = 0$.

smaller (by almost two orders of magnitude according to Ref. [38]) than the pn breakup cross section.

Note that the factors C and β introduce an additional uncertainty in the estimation of the magnitude of the pp breakup cross section. While the factor C can be evaluated in the quark-interchange model thus staying within the framework of the considered model, the factor β is not constrained by the theoretical framework of the model. The latter is sensitive to the angular dependence, $F(\theta_{\rm c.m.})$, of the helicity amplitudes. To estimate the uncertainty due to $F(\theta_{\rm c.m.})$ we varied it around the form $F(\theta_{\rm c.m.}) = \frac{1}{\sin^2(\theta_{\rm c.m.})(1-\cos(\theta_{\rm c.m.}))^2}$ in such a way that the results were still in agreement with angular distribution of pp scattering at $-t, -u > 1$ GeV^2. We found that this variation changes the HRM prediction for the magnitude of pp breakup cross section as much as 40%.

Because the pp breakup cross section is still by a factor of 10 smaller than the pn cross section, one needs to estimate the contribution due to three-body processes in which hard pn breakup is followed by soft charge-exchange rescattering. The estimate based on Eq. (45) is given in Fig. 6 where the ratio of three-body to two-body breakup cross sections is evaluated for different values of α_s and transverse momentum of the spectator neutron, $p_{s\perp}$.

Because of the eikonal nature of the second rescattering in three-body processes, one expects the cross section to be maximal at $\alpha_s = 1$. As Fig. 6(a) shows in this case, the three-body process is a correction to the two-body breakup process, $\sim$2% for $p_{s\perp} = 100$ MeV/c and $\sim$17% for $p_{s\perp} = 200$ MeV/c. Then, starting at $p_{s\perp} > 300$ MeV/c the three-body process dominates the two-body contribution. The latter can be verified by observing an onset of s^{-12} scaling at large ($\geqslant$300 MeV/c) transverse momenta of the spectator neutron in the case of hard pp breakup reactions. Fig. 6(b) shows also that the three-body contribution will be always small for $p_{s\perp} \approx 0$ MeV/c, and for a wide range of α_s, which again reflects the eikonal nature of the second order rescattering in which case the recoiling of the spectator nucleons happens predominantly at $\sim$90° (see, e.g., Ref. [49]). Note that one expects the above estimate of the three-body contribution to contain an uncertainty of 10–15%, representing the general level of accuracy of eikonal approximations.

Based on Fig. 6 one can expect that, overall, for small values of $p_s \leqslant 100$–150 MeV/c in the high energy limit ($E_\gamma > 2$ GeV) one expects two-body breakup mechanisms to dominate for both pp and pn production reactions.

B. Spectator nucleon momentum dependence

The presence of a spectator nucleon in the hard two-nucleon breakup reaction from ^{3}He gives us an additional degree of freedom in checking the mechanism of the photodisintegration. As follows from Eqs. (34) and (35) and Eqs. (41) and (43) the pn and pp breakup cross sections within HRM are sensitive to different components of the nuclear spectral function. This is due to the fact that the pp component with the same helicities for both protons is suppressed in the ground state wave function of the ^{3}He target. Thus one expects rather different spectator-momentum dependencies for pp and pn breakup cross sections.

The quantity that we consider for numerical estimates is not the momentum of the spectator but rather the momentum fraction of the target carried by the spectator nucleon, α_s. This quantity is Lorentz invariant with respect to boosts in the q direction, which allows us to specify it in the Lab frame as follows:

$$\alpha_s \equiv \frac{E_s - p_{s,z}}{M_A/A} = \alpha_A - \alpha_{1f} - \alpha_{2f}, \qquad (50)$$

where $\alpha_i = \frac{E_i - p_{i,z}}{M_A/A}$ for $i = A, 1f, 2f$ and z axis in the Lab frame is defined parallel to the momentum of incoming photon q. Note that the photon does not contribute to the above equation because $\alpha_q = 0$. In definition of α_s we use a normalization such that for a stationary spectator $\alpha_s = 1$. The α_s dependencies of the differential cross sections for pp and pn breakup reactions normalized to their values at $\alpha_s = 1$ are given in Fig. 7(a). One feature of α_s dependence is the asymmetry of the cross section around $\alpha_s = 1$ with cross sections dominating at $\alpha_s > 1$. This property can be understood from the fact that the momentum fraction of the NN pair that breaks up is defined through α_s as follows:

$$\alpha_{NN} = 3 - \alpha_s. \qquad (51)$$

The latter quantity defines the invariant energy of the NN pair as follows:

$$s_{NN} = M_{NN}^2 + E_\gamma m_n \alpha_{NN}. \qquad (52)$$

Because the cross section within the HRM is proportional to s_{NN}^{-10},[5] it will be enhanced at small values of s_{NN} that will correspond to smaller values of α_{NN} or larger values of α_s.

[5] An additional negative power of invariant energy is provided by the $\frac{1}{s-M_A^2}$ factor in the differential cross section of the reaction [see Eqs. (34), (41)].

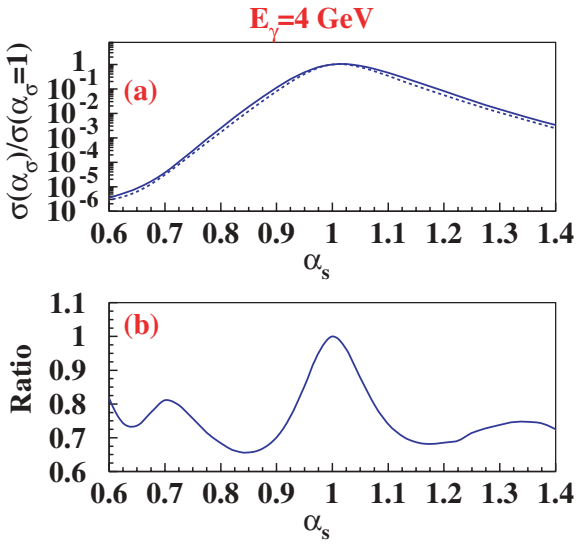

FIG. 7. (Color online) Dependence of the s^{11} weighted 90° c.m. breakup differential cross section on the light-cone momentum fraction of the spectator nucleon, α_s, calculated at $E_\gamma = 4$ GeV and $p_{s\perp} = 0$. (a) The solid line is for pp breakup reactions, and the dashed line is for pn breakup reactions. Calculations are normalized to the cross sections at $\alpha_s = 1$. (b) Ratio of the pn to pp breakup cross sections normalized to their values at $\alpha_s = 1$.

The difference of the cross sections due to the different composition of the nuclear spectral functions entering the pp and pn breakup reactions can be seen in Fig. 7(b) in which case one calculates the ratio of pn to pp breakup cross sections normalized to their values at $\alpha_s = 1$. The drop of the ratio in Fig. 7(b) at values close to $\alpha_s = 1$ is due to the suppression of the same-helicity two-proton component in the ground state nuclear wave function at small momenta. In this case the spectral function is sensitive to the higher angular momentum components of the ground state nuclear wave function. This yields a wider momentum distribution for the pp spectral function as compared to that for pn because no same-helicity state suppression exits for the latter. The estimates indicate that differences in α_s dependencies of pp and pn breakup cross sections are rather large and can play an additional role in checking the validity of the HRM.

VII. POLARIZATION TRANSFER OF THE HARD RESCATTERING MECHANISM

One of the unique properties of the hard rescattering mechanism of two-nucleon breakup is that the helicity of the nucleon from which a quark is struck is predominantly defined by the helicity of the incoming photon $\lambda_{1i} = \lambda_\gamma$ [see Eq. (18)]. This is based on the fact that in the massless quark limit the helicity of the struck quark equals the helicity of the photon, $\eta_{1i} = \lambda_\gamma$, and assuming that at large x the quark carries almost all the helicity of the parent nucleon one obtains $\lambda_{1i} \approx \eta_{1i} = \lambda_\gamma$.

Because within the HRM, the energetic struck quark shares its momentum with a quark of the other nucleon through a hard gluon exchange, it will retain its initial helicity when it merges into the final outgoing nucleon. It will also have $x' \sim x \sim 1$, which allows us to conclude that the final outgoing nucleon will acquire the large part of struck quark's (as well as the photon's) helicity. This mechanism will result in a large (photon) polarization transfer for the hard two-nucleon breakup reactions.

An observable that is sensitive to polarization transfer processes is the quantity $C_{z'}$, which for a circularly polarized photon measures the asymmetry of the hard breakup reaction with respect to the helicity of the outgoing proton.

A large value of $C_{z'}$ was predicted within the HRM for the hard breakup of the deuteron in Ref. [25] that was observed in the recent experiment of Ref. [12].

For the case of the ^{3}He target an additional experimental observation will be a comparison of $C_{z'}$ asymmetries for pp and pn breakup channels. For the ^{3}He target we define $C_{z'}$ as follows:

$$C_{z'} = \frac{\sum_{\lambda_{2f},\lambda_s,\lambda_a}\{|\langle +,\lambda_{2f},\lambda_s|M|+,\lambda_A\rangle|^2 - |\langle -,\lambda_{2f},\lambda_s|M|+,\lambda_A\rangle|^2\}}{\sum_{\lambda_{1f}\lambda_{2f},\lambda_s,\lambda_a}|\langle \lambda_{1f},\lambda_{2f},\lambda_s|M|+,\lambda_A\rangle|^2}. \tag{53}$$

Using Eq. (18) and the definitions of Eq. (24) for $C_{z'}$ one obtains

$$C_{z'} = \frac{(|\phi_1|^2 - |\phi_2|^2)S^{++} + (|\phi_3|^2 - |\phi_4|^2)S^{+-}}{2|\phi_5|^2 S^+ + (|\phi_1|^2 + |\phi_2|^2)S^{++} + (|\phi_3|^2 + |\phi_4|^2)S^{+-}}, \tag{54}$$

where

$$S^{\pm,\pm}(t_1,t_2,\alpha,\vec{p}_s) = \sum_{\lambda_A=-\frac{1}{2}}^{\frac{1}{2}}\sum_{\lambda_3=-\frac{1}{2}}^{\frac{1}{2}}\left|\int \Psi^{\lambda_A}_{^3\mathrm{He,NR}} \times \left(\vec{p}_1,\lambda_1=\pm\frac{1}{2},t_1;\vec{p}_2,\lambda_2=\pm\frac{1}{2},t_2;\vec{p}_s,\lambda_3\right) \times m_N\frac{d^2p_{2,\perp}}{(2\pi)^2}\right|^2 \tag{55}$$

and $S^+ = S^{++} + S^{+-}$.

As follows from Eqs. (54) and (55), one predicts significantly different magnitudes for $C_{z'}$ for pp and pn breakup cases.

For the pp breakup, $S_{pp}^{++} \ll S_{pp}^{+-}$ due to the smallness of the nuclear wave function component containing two protons in the same helicity state. As a result one expects

$$C_{z'}^{pp} \approx \frac{|\phi_3|^2 - |\phi_4|^2}{|\phi_3|^2 + |\phi_4|^2} \sim 0, \tag{56}$$

while for the pn breakup case $S_{pn}^{++} \approx S_{pn}^{+-}$, then one obtains

$$C_{z'}^{pn} \approx \frac{|\phi_1|^2 + |\phi_3|^2 - |\phi_4|^2}{|\phi_1|^2 + |\phi_3|^2 + |\phi_4|^2} \sim \frac{2}{3}, \tag{57}$$

where in the last part of the equation we assumed that $|\phi_3| = |\phi_4| = \frac{1}{2}|\phi_1|$.

VIII. CONCLUSIONS

The hard rescattering mechanism of a two-nucleon breakup from the ^{3}He nucleus at large c.m. angles is based on the assumption of the dominance of quark-gluon degrees of freedom in the hard scattering process involving two nucleons. The model explicitly assumes that the photodisintegration process proceeds through the knock-out of a quark from one nucleon with a subsequent rescattering of that quark with a quark from the second nucleon. While photon-quark scattering is calculated explicitly, the sum of all possible quark rescatterings is related to the hard elastic NN scattering amplitude. Such a relation is found assuming that quark-interchange amplitudes give the dominant contribution in the hard elastic NN scattering.

The model allows one to calculate the cross sections of the hard breakup of pn and pp pairs from ^{3}He expressing them through the amplitudes of elastic pn and pp scatterings, respectively.

Several results of the HRM are worth mentioning: First, the HRM predicts an approximate s^{-11} scaling consistent with the predictions of the quark-counting rule. However, the model by itself is nonperturbative because the bulk of the incalculable part of the scattering amplitude is hidden in the amplitude of the NN scattering that is taken from the experiment.

Second, because the hard NN scattering amplitude enters into the final amplitude of the photodisintegration reaction, the shape of the energy dependence of the s^{11} weighted breakup cross section reflects the shape of the s^{10} weighted NN elastic scattering cross section. Because of a better accuracy of pp elastic scattering data for $s_{NN} \leqslant 24$ GeV^2, we are able to predict a specific shape for the energy dependence of the hard pp breakup cross section at photon energies up to $E_\gamma \leqslant 5$ GeV.

Another observations is that, when s^{-11} scaling is established, the HRM predicts an increase of the strength of the pp breakup cross section relative to the pn breakup as compared to the low energy results. This is due to the feature that within the quark-interchange mechanism of NN scattering one has more charges flowing between nucleons in the pp pair than in the pn pair. This situation is opposite in the low energy regime when no charged meson exchanges exist for the pp pair. Even though the large charge factor is involved in the pp breakup its cross section is still by a factor of ten smaller than the cross section of the pn breakup. Within the HRM, this is due to cancellation between the helicity conserving amplitudes ϕ_3 and ϕ_4, which have opposite signs for the pp scattering.

Because of the smallness of the pp breakup cross section, within the eikonal approximation, we estimated the possible contribution of three-body/two-step processes in which the initial two-body hard pn breakup is followed by the charge-exchange rescattering of an energetic neutron off the spectator proton. We found that this contribution has s^{-12} energy dependence and is a small correction for spectator nucleon momenta $\leqslant$150 MeV/c. However, the three-body/two-step process will dominate the hard pp breakup contribution at large transverse momenta of the spectator nucleon starting at $p_{s\perp} \geqslant 350$ MeV/c.

The next result of the HRM is the prediction of different spectator-momentum dependencies of breakup cross section for the pp and pn pairs. This result follows from the fact that the ground state wave function of ^{3}He containing two protons with the same helicity is significantly suppressed as compared to the same component in the pn pair. Because of this, the pp spectral function is sensitive to the higher angular momentum components of the nuclear ground state wave function. These components generate wider momentum distribution as compared to say the S component of the wave function. As a result the cross section of the pp breakup reaction exhibits wider momentum distribution as compared to the pn cross section. Additionally because of the strong s dependence of the reaction, the cross section exhibits an asymmetry in the light-cone momentum distribution of the spectator nucleon, favoring larger values of α_s.

The final result of the HRM is the strong difference in prediction of the polarization transfer asymmetry for pp and pn breakup reactions for circularly polarized photons. Because of the suppression of the same helicity pp components in the ^{3}He ground state wave function, the dominant helicity conserving ϕ_1 component will not contribute to the polarization transfer process involving two protons. Because of this effect, the HRM predicts longitudinal polarization transfer $C_{z'}$, for the pp breakup to be close to zero. Because no such suppression exists for the pn breakup, the HRM predicts a rather large magnitude for $C_{z'} \approx \frac{2}{3}$.

Even though the HRM model does not contain free parameters, for numerical estimates we use the magnitude of elastic NN cross sections as well as some properties of the NN helicity amplitudes. This introduces certain error in our prediction of the magnitudes of the breakup cross sections. For the pn breakup this error is mainly related to the uncertainty in the magnitude of the absolute cross section of hard elastic pn scattering which is on the level 30%. For the pp breakup the main source of the uncertainty is the magnitude of the cancellation between ϕ_3 and ϕ_4, which is sensitive to the angular distribution of helicity amplitudes. The uncertainty due to the angular function is on the level of 40%. These uncertainties should be considered on top of the theoretical uncertainties that the HRM contains due to approximations such as estimating the scattering amplitude at maximal value of the nuclear wave function at $\alpha = \frac{1}{2}$. The latter may introduce an uncertainty of as much as 20% in the breakup cross section.

In conclusion we expect that experimental verification of all the above-mentioned predictions may help us to verify the

validity of the hard rescattering model. Also, the progress in extracting the helicity amplitudes of the hard NN scattering will allow us to improve the accuracy of HRM predictions.

ACKNOWLEDGMENTS

We are grateful to Drs. Ronald Gilman, Leonid Frankfurt, Eli Piasetzky, and Mark Strikman for many useful discussions and comments. Special thanks to Drs. Ronald Gilman, Eli Piasetzky, and Ishay Pomerantz for the discussion of their experimental results that allowed us to find the cancellation factor in the pp breakup cross section, which was overlooked in our calculations earlier. This work is supported by US Department of Energy Grant under Contract DE-FG02-01ER41172.

APPENDIX A: CALCULATION OF THE ^{3}He$(\gamma, NN)N$ SCATTERING AMPLITUDE

Applying Feynman diagram rules for the scattering amplitude corresponding to the diagram of Fig. 1(a) one obtains

$$
\begin{aligned}
&\langle \lambda_{f1}, \lambda_{f2}, \lambda_s | A | \lambda_\gamma, \lambda_A \rangle \\
&= (N1): \int \frac{-i\Gamma_{N_{1f}} i[\not{p}_{1f} - \not{k}_1 + m_q]}{(p_{1f} - k_1)^2 - m_q^2 + i\epsilon} i S(k_1) \\
&\quad \cdots [-igT_c^F \gamma_\mu] \cdots \frac{i[\not{p}_{1i} - \not{k}_1 + m_q](-i)\Gamma_{N_{1i}}}{(p_{1i} - k_1)^2 - m^2 + i\epsilon} \frac{d^4k_1}{(2\pi)^4} \\
&\quad \times (\gamma q): \frac{i[\not{p}_{1i} - \not{k}_1 + \not{q} + m_q]}{(p_{1i} - k_1 + q)^2 - m_q^2 + i\epsilon} [-iQ_i e \epsilon^\perp \gamma^\perp] \\
&\quad (N2): \int \frac{-i\Gamma_{N_{2f}} i[\not{p}_{2f} - \not{k}_2 + m_q]}{(p_{2f} - k_2)^2 - m_q^2 + i\epsilon} i S(k_2) \\
&\quad \cdots [-igT_c^F \gamma_\nu] \frac{i[\not{p}_{2i} - \not{k}_2 + m_q](-i)\Gamma_{N_{2i}}}{(p_{2i} - k_2)^2 - m^2 + \epsilon} \frac{d^4k_2}{(2\pi)^4} \\
&\quad (^3\mathrm{He}): \int \frac{-i\Gamma_{^3\mathrm{He}} \cdot \bar{u}_{\lambda_s}(p_s) i[\not{p}_{NN} - \not{p}_{2i} + m_N]}{(p_{NN} - p_{2i})^2 - m_N^2 + i\epsilon} \\
&\quad \times \frac{i[\not{p}_{2i} + m_N]}{p_{2i}^2 - m_N^2 + i\epsilon} \frac{d^4p_{2i}}{(2\pi)^4} \\
&\quad (g): \frac{id^{\mu,\nu}\delta_{ab}}{[(p_{2i} - k_2) - (p_{1i} - k_1) - (q - l)]^2 + i\epsilon},
\end{aligned}
\tag{A1}
$$

where the momenta involved above are defined in Fig. 1. Note that the terms above are grouped according to their momenta. As such they do not represent the correct sequence of the scattering presented in Fig. 1. To indicate this we separated the disconnected terms by "...".

The covariant vertex function $\Gamma_{^3\mathrm{He}}$ describes the transition of the ^{3}He nucleus to a three-nucleon system. The vertex function Γ_N describes a transition of a nucleon to one-quark and a residual spectator quark-gluon system with total momentum $k_i, (i = 1, 2)$. The function $S(k)$ describes the propagation of the off-mass shell quark-gluon spectator system of the nucleon. As is shown below, this nonperturbative function can be included in the definition of a nonperturbative single quark wave function of the nucleon.

Using the reference frame and the kinematic conditions described in Sec. II we now elaborate each labeled term of Eq. (A1) separately.

(^{3}He). Using the light-cone representation of four-momenta and introducing the light-cone momentum fraction of the NN pair carried by the nucleon $2i$ as $\alpha = \frac{p_{2i+}}{p_{NN+}}$, one represents the nucleon propagators as well as the momentum integration d^4p_{2i} in the following form:

$$
\begin{aligned}
p_{2i}^2 - m_N^2 + i\epsilon &= \alpha \cdot p_{NN+} \left(p_{2i-} - \frac{m_N^2 + p_{2i\perp}^2}{\alpha p_{NN+}} \right) \\
&\quad + i\epsilon \\
(p_{NN} - p_{2i})^2 - m_N^2 + i\epsilon &= p_{NN+}(1-\alpha) \left(\frac{M_{NN}^2}{p_{NN+}} - p_{2i-} \right) \\
&\quad - \left(m_N^2 + p_{i\perp}^2 \right) + i\epsilon \\
d^4p_{2i} &= p_{NN+} \frac{1}{2} d\alpha dp_{2i-} d^2p_{2i\perp}.
\end{aligned}
\tag{A2}
$$

Using these relations in Eq. (A1) we can integrate over dp_{2i-} taking the residue at the pole of the $(2i)$-nucleon propagator, i.e.,

$$
\int \frac{[\cdots] dp_{2i-}}{p_{2i-} - \frac{m_N^2 + p_{2i\perp}^2}{\alpha p_{NN+}} + i\epsilon} = -2\pi i [\cdots]|_{p_{2i-} = \frac{m_N^2 + p_{2i\perp}^2}{\alpha p_{NN+}}}. \tag{A3}
$$

After this integration one can use the following relations in Eq. (A1):

$$
\begin{aligned}
\not{p}_{2i} + m_N &= \sum_{\lambda_{2i}} u_{\lambda_{2i}}(p_{2i}) \bar{u}_{\lambda_{2i}}(p_{2i}) \\
(p_{NN} - p_{2i})^2 - m_N^2 &= (1-\alpha) \left(M_{NN}^2 - \frac{m_N^2 + p_{2i\perp}^2}{\alpha(1-\alpha)} \right) \\
\not{p}_{NN} - \not{p}_{2i} + m_N &= \sum_{\lambda_{1i}} u_{\lambda_{1i}}(p_{1i}) \bar{u}_{\lambda_{1i}}(p_{1i}) \\
&\quad + \frac{M_{NN}^2 - \frac{m_N^2 + p_{2i\perp}^2}{\alpha(1-\alpha)}}{2p_{NN+}} \gamma^+.
\end{aligned}
\tag{A4}
$$

Furthermore we use the condition $p_{NN+}^2 \gg \frac{1}{2}(M_{NN}^2 - \frac{m_N^2 + p_{2i\perp}^2}{\alpha(1-\alpha)})$ to neglect the second term of the right-hand part of the third equation in Eq. (A4). This relation is justified for the high energy kinematics described in Sec. II as well as from the fact that in the discussed model the scattering amplitude is defined at $\alpha \approx \frac{1}{2}$.

Introducing the light-cone wave function of ^{3}He [30,31,50],

$$
\Psi_{^3\mathrm{He}}^{\lambda_A, \lambda_1, \lambda_2, \lambda_s}(\alpha, p_\perp) = \frac{\Gamma_{^3\mathrm{He}}^{\lambda_A} \bar{u}_{\lambda_1}(p_{NN} - p) \bar{u}_{\lambda_2}(p) \bar{u}_{\lambda_s}(p_s)}{M_{NN}^2 - \frac{m_N^2 + p_\perp^2}{\alpha(1-\alpha)}},
\tag{A5}
$$

and collecting all the terms of Eq. (A4) in the (^{3}He:) part of Eq. (A1) one obtains

$$(^3\mathrm{He}:) = \sum_{\lambda_{1i},\lambda_{i2}} \int \frac{\Psi^{\lambda_A,\lambda_{i1},\lambda_{i2},\lambda_s}_{^3\mathrm{He}}(\alpha,\, p_{i\perp})}{1-\alpha} \times u_{\lambda_{i1}}(p_1) u_{\lambda_{i2}}(p_2) \frac{d\alpha}{\alpha} \frac{d^2 p_{2i\perp}}{2(2\pi)^3}. \tag{A6}$$

(N1:). To evaluate this term in Eq. (A1) we first introduce

$$\begin{aligned} x_1 &= \frac{k_{1+}}{p_{1i+}} = \frac{k_{1+}}{(1-\alpha)p_{NN+}}, \\ x_1' &= \frac{k_{1+}}{p_{1f+}} = \frac{1-\alpha}{1-\alpha'} x_1, \end{aligned} \tag{A7}$$

where $\alpha' = \frac{p_{2f+}}{p_{NN+}}$. Furthermore we perform the k_{1-} integration such that it puts the spectator system of the $N1$ nucleon at its on-mass shell. This results in

$$\int S(k_1) dk_{1-} = -\frac{2\pi i}{p_{1+}x_1} \sum_s \psi_s(k_1)\psi_s^\dagger(k_1)\big|_{k_{1-}=\frac{m_s^2+k_{1\perp}^2}{p_{1+}x_1}}, \tag{A8}$$

where $\psi_s(k)$ represents the nucleon's spectator wave function with mass m_s and spin s. Note that in the definition of ψ_s one assumes an integration over all the internal momenta of the spectator system. Using Eq. (A8) for the (N1) term one obtains

$$\begin{aligned} (N1):& \sum_s \int \frac{-i\Gamma_{N_{1f}} i(\not{p}_{1f} - \not{k}_1 + m_q)}{(p_{1f}-k_1)^2 - m_q^2 + i\epsilon} \psi_s(k_1) \cdots \\ &\cdots \big[-igT_c^F \gamma_\mu\big] \psi_s^\dagger(k_1) \frac{i(\not{p}_{1i} - \not{k}_1 + m_q)(-i)\Gamma_{N_{1i}}}{(p_{1i}-k_1)^2 - m^2 + i\epsilon} \\ &\times \frac{dx_1}{x_1} \frac{d^2 k_{1\perp}}{2(2\pi)^3}. \end{aligned} \tag{A9}$$

Now we evaluate the propagator of the off-shell quark with the momentum $p_{1i} - k_1$. This yields

$$\begin{aligned} &\frac{\not{p}_{1i} - \not{k}_1 + m_q}{(p_{1i}-k_1)^2 - m_q^2} \\ &= \frac{(\not{p}_{1i} - \not{k}_1)^{\text{on shell}} + m_q}{(1-x_1)\big(\tilde{m}_{N1}^2 - \frac{m_s^2(1-x_1)+m_q^2 x_1 + (k_{1\perp} - x_1 p_{1\perp})^2}{x_1(1-x_1)}\big)} \\ &\quad + \frac{\gamma^+}{2(1-\alpha)(1-x_1)p_{NN+}}, \end{aligned} \tag{A10}$$

where the effective off-shell mass of the nucleon is defined as

$$\tilde{m}_N^2 = \frac{M_{NN}^2 \alpha(1-\alpha) - m_N^2(1-\alpha) - p_\perp^2}{\alpha}. \tag{A11}$$

As it follows from Eq. (A10) at the high energy limit, $p_{NN+}^2 \gg m_N^2$, one can neglect the second term of the RHS (off-shell) part of the equation if $(1-\alpha)(1-x_1) \sim 1$. As is shown in Sec. II [see discussion before Eq. (12)], the essential values that contribute in the scattering amplitude correspond to $\alpha \approx \frac{1}{2}$ and $(1-x_1) \sim 1$. Therefore the second term in the right-hand side of Eq. (A10) can be neglected. Using the closure relation for the on-shell spinors for Eq. (A10) one obtains

$$\begin{aligned} &\frac{\not{p}_{1i} - \not{k}_1 + m_q}{(p_{1i}-k_1)^2 - m_q^2} \\ &= \frac{\sum_{\eta_{1i}} u_{\eta_{1i}}(p_{1i}-k_1)\bar{u}_{\eta_{1i}}(p_{1i}-k_1)}{(1-x_1)\big(\tilde{m}_{N1}^2 - \frac{m_s^2(1-x_1)+m_q^2 x_1 + (k_{1\perp} - x_1 p_{1\perp})^2}{x_1(1-x_1)}\big)}. \end{aligned} \tag{A12}$$

Similar considerations yield the following expression for the propagator of the quark entering the wave function of the final nucleon "1f":

$$\begin{aligned} &\frac{\not{p}_{1f} - \not{k}_1 + m_q}{(p_{1f}-k_1)^2 - m_q^2} \\ &= \frac{\sum_{\eta_{1f}} u_{\eta_{1f}}(p_{1f}-k_1)\bar{u}_{\eta_{1f}}(p_{1f}-k_1)}{(1-x_1')\big(m_N^2 - \frac{m_s^2(1-x_1')+m_q^2 x_1' + (k_{1\perp} - x_1' p_{1f\perp})^2}{x_1'(1-x_1')}\big)}, \end{aligned} \tag{A13}$$

where x_1' is defined in Eq. (A7).

By inserting Eqs. (A12) and (A13) into Eq. (A9) and defining the quark wave function of the nucleon as

$$\Psi_N^{\lambda,\eta}(p,x,k_\perp) = \frac{u_N^\lambda(p)\Gamma_N \bar{u}_\eta(p-k)\psi_s^\dagger(k)}{m_N^2 - \frac{m_s^2(1-x)+m_q^2 x + (k_\perp - x p_\perp)^2}{x(1-x)}}, \tag{A14}$$

for the ($N1$:) term we obtain

$$\begin{aligned} (N1:)& \sum_{\eta_{1f},\eta_{1i},s_1} \int \frac{\Psi^{\dagger\lambda_{1f},\eta_{1f}}(p_{1f},x_1',k_{1\perp})}{(1-x_1')} \bar{u}_{\eta_{1f}}(p_{1f}-k_1)\cdots \\ &\cdots[-igT_c^F\gamma_\mu] u_{\eta_{1i}}(p_{1i}-k_1) \frac{\Psi^{\lambda_{1i},\eta_{1i}}(p_{1i},x_1,k_{1\perp})}{(1-x_1)} \\ &\times \frac{dx_1}{x_1} \frac{d^2 k_{1\perp}}{2(2\pi)^3}. \end{aligned} \tag{A15}$$

(N2:). This term can be evaluated following similar considerations used above in the evaluation of the (N1:) term. Introducing light-cone momentum fraction of the spectator system of the second nucleon as

$$\begin{aligned} x_2 &= \frac{k_{2+}}{p_{2i+}} = \frac{k_{2+}}{\alpha p_{NN+}}, \\ x_2' &= \frac{k_{2+}}{p_{2f+}} = \frac{\alpha}{\alpha'} x_2, \end{aligned} \tag{A16}$$

for the (N2:) term we obtain

$$\begin{aligned} (N2:)& \sum_{\eta_{2f},\eta_{2i},s_2} \int \frac{\Psi^{\dagger\lambda_{2f},\eta_{2f}}(p_{2f},x_2',k_{2\perp})}{(1-x_2')} \bar{u}_{\eta_{2f}}(p_{2f}-k_2)\cdots \\ &\cdots u_{\eta_{2i}}(p_{2i}-k_2) \frac{\Psi^{\lambda_{2i},\eta_{2i}}(p_{2i},x_2,k_{2\perp})}{(1-x_2)} \\ &\times \frac{dx_2}{x_2} \frac{d^2 k_{2\perp}}{2(2\pi)^3}. \end{aligned} \tag{A17}$$

Collecting the expressions of Eqs. (A6), (A15), and (A17) in Eq. (A1) and rearranging terms to express the sequence of the scattering, we obtain the expression of the scattering amplitude presented in Eq. (7).

APPENDIX B: CALCULATION OF THE NUCLEON-NUCLEON SCATTERING AMPLITUDE

In this section we consider a hard NN elastic scattering model in which two nucleons interact through the QIM. The typical diagram for such scattering is presented in Fig. 8. Applying Feynman diagram rules for these diagrams one obtains

$$\begin{aligned} A_{NN}^{\rm QIM} &= (N1): \int \frac{-i\Gamma_{N_{1f}} i[\not p_{1f} - \not k_1 + m_q]}{(p_{1f}-k_1)^2 - m_q^2 + i\epsilon} iS(k_1) \\ &\cdots \left[-igT_c^F \gamma_\mu\right] \frac{i[\not p_{1i}^* - \not k_1 + m_q](-i)\Gamma_{N_{1i}}}{(p_{1i}^*-k_1)^2 - m^2 + i\epsilon} \frac{d^4k_1}{(2\pi)^4} \\ &(N2): \int \frac{-i\Gamma_{N_{2f}} i[\not p_{2f} - \not k_2 + m_q]}{(p_{2f}-k_2)^2 - m_q^2 + i\epsilon} S(k_2) \\ &\cdots \left[-igT_c^F \gamma_\nu\right] \frac{i[\not p_{2i} - \not k_2 + m_q](-i)\Gamma_{N_{2i}}}{(p_{2i}-k_2)^2 - m^2 + \epsilon} \frac{d^4k_2}{(2\pi)^4} \\ &(g): \frac{id^{\mu,\nu}\delta_{ab}}{r^2+i\epsilon} - (p_{1f} \leftrightarrow p_{2f}), \end{aligned} \tag{B1}$$

where definitions of the momenta are given in Fig. (8). The procedure of reducing the above amplitude is similar to the one used in the previous section. First we estimate the propagators of each nucleon's spectator system at their pole values, $k_{i,-} = \frac{m_s^2+k_{i,\perp}^2}{x_i p^+} (i = 1, 2)$, by performing the $k_{i,-}$ integration, which yields

$$\int [\cdots] S(k_i) dk_{i-} = -\frac{2\pi i [\cdots]}{x_i p_+} \sum_s \psi_s(k_i)\psi_s^\dagger(k_i)\Big|_{k_{i,-}=\frac{m_s^2+k_{i,\perp}^2}{x_i p_+}}. \tag{B2}$$

Furthermore, because $p_+^2 \gg m_N^2$ one can apply, similar to Eqs. (A12) and (A13), approximations for propagators of interchanging quarks leaving and entering the corresponding nucleons. Then using the definition of single quark wave function according to Eq. (A14) for the (N_1) and (N_2) terms, one obtains similar expressions that can be presented in the following form:

$$\begin{aligned} (N1:) &\sum_{\eta_{1,2f},\eta_{2,1i},s} \int \frac{\Psi^{\dagger\lambda_{1f},\eta_{1f}}(p_{1f}, x_1', k_{1\perp})}{(1-x_1')} \bar u_{\eta_{1f}}(p_{1f}-k_1)\cdots \\ &\cdots [-igT_c^F\gamma_\mu] u_{\eta_{1i}}(p_{1i}^*-k_1) \frac{\Psi^{\lambda_{1i},\eta_{i1}}(p_{1i}, x_1, k_{1\perp})}{(1-x_1)} \\ &\times \frac{dx_1}{x_1}\frac{d^2k_{1\perp}}{2(2\pi)^3}. \end{aligned} \tag{B3}$$

The $(N2:)$ term is obtained from the above equation by replacing $1 \to 2$. Regrouping (N1) and (N2) terms given by Eq. (B3) into Eq. (B1), for the amplitude of nucleon-nucleon scattering in QIM we obtain

$$\begin{aligned} A_{NN}^{\rm QIM} = \sum_{\eta_{1i}\eta_{2i}\eta_{1f}\eta_{2f}} \int \Bigg[&\left\{ \frac{\psi_N^{\dagger\lambda_{2f},\eta_{2f}}(p_{2f}, x_2', k_{2\perp})}{1-x_2'} \bar u_{\eta_{2f}} \right. \\ &(p_{2f}-k_2)\left[-igT_c^F\gamma^\nu\right] u_{\eta_{1i}}(p_{1i}^*-k_1) \\ &\left. \times \frac{\psi_N^{\lambda_{1i},\eta_{1i}}(p_{1i}^*, x_1, k_{1\perp})}{(1-x_1)} \right\} \\ &\times \left\{ \frac{\psi_N^{\dagger\lambda_{1f},\eta_{1f}}(p_{1f}, x_1', k_{1\perp})}{1-x_1'} \bar u_{\eta_{1f}}(p_{1f}-k_1) \right. \\ &\left. \times \left[-igT_c^F\gamma^\mu\right] u_{\eta_{2i}}(p_{2i}-k_2) \frac{\psi_N^{\lambda_{2i},\eta_{2i}}(p_{2i}, x_2, k_{2\perp})}{(1-x_2)} \right\} \\ &\times G^{\mu,\nu}(r) \frac{dx_1}{x_1}\frac{d^2k_{1\perp}}{2(2\pi)^3}\frac{dx_2}{x_2}\frac{d^2k_{2\perp}}{2(2\pi)^3} \Bigg]. \end{aligned} \tag{B4}$$

Note that in the above expression we redefined the initial momentum of the "$N1$" nucleon to p_{1i}^* to emphasize its difference from p_{1i}, which enters in the photodisintegration amplitude. In the latter case p_{1i} is not independent and it is defined by the momenta of the two remaining nucleons in the ^{3}He nucleus.

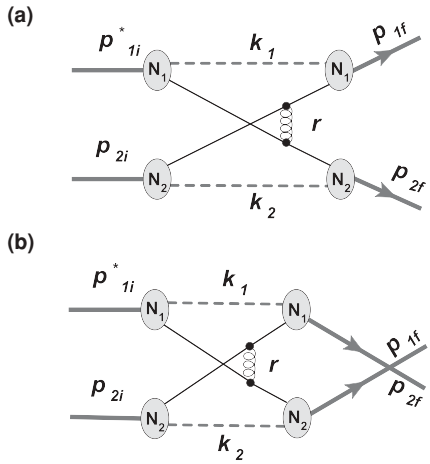

FIG. 8. Quark interchange contribution to nucleon-nucleon scattering.

APPENDIX C: CALCULATION OF QUARK-CHARGE FACTORS IN QIM MODEL OF NN SCATTERING

We consider now the hard elastic NN scattering (described through $a + b \to c + d$ reaction) within quark-interchange approximation following the approach used in Ref. [35]. In this case one can represent the scattering amplitude as follows:

$$\begin{aligned} &\langle cd|T|ab\rangle \\ &= \sum_{\alpha,\beta,\gamma} \langle\psi_c^\dagger|\alpha_2',\beta_1',\gamma_1'\rangle\langle\psi_d^\dagger|\alpha_1',\beta_2',\gamma_2'\rangle \\ &\quad\times\langle\alpha_2',\beta_2',\gamma_2',\alpha_1'\beta_1'\gamma_1'|H|\alpha_1,\beta_1,\gamma_1,\alpha_2\beta_2\gamma_2\rangle \\ &\quad\cdot\langle\alpha_1,\beta_1,\gamma_1|\psi_a\rangle\langle\alpha_2,\beta_2,\gamma_2|\psi_b\rangle, \end{aligned} \tag{C1}$$

where (α_i, α_i'), (β_i, β_i'), and $(\gamma_i\gamma_i')$ describe the spin-flavor quark states before and after the hard scattering, H, and

$$C_{\alpha,\beta,\gamma}^j = \langle\alpha,\beta,\gamma|\psi_j\rangle \tag{C2}$$

describes the probability amplitude of finding an α, β, γ helicity-flavor combination of three valence quarks in the

nucleon j. The $C^j_{\alpha,\beta,\gamma}$ terms can be calculated by representing the nucleon wave functions on the helicity-flavor basis. For SU(6) symmetric wave function such representation reads

$$\psi^{i^3_N,h_N} = \frac{1}{\sqrt{2}}\Big\{\big(\chi^{(23)}_{0,0}\chi^{(1)}_{\frac{1}{2},h_N}\big)\cdot\big(\tau^{(23)}_{0,0}\tau^{(1)}_{\frac{1}{2},i^3_N}\big) + \sum_{i^3_{23}=-1}^{1}\sum_{h^3_{23}=-1}^{1}\left\langle 1,h_{23};\frac{1}{2},h_N-h_{23}\middle|\frac{1}{2},h_N\right\rangle \times\left\langle 1,i^3_{23};\frac{1}{2},i^3_N-i^3_{23}\middle|\frac{1}{2},i^3_N\right\rangle \times\big(\chi^{(23)}_{1,h_{23}}\chi^{(1)}_{\frac{1}{2},h_N-h_{23}}\big)\cdot\big(\tau^{(23)}_{1,i^3_{23}}\tau^{(1)}_{\frac{1}{2},i^3_N-i^3_{23}}\big)\Big\}, \quad \text{(C3)}$$

where we separated the wave function into two parts with two quarks (e.g., 2nd and 3rd) being in helicity zero-isosinglet and helicity one-isotriplet states. Here $\chi_{j,h}$ is the helicity wave function with total spin j and helicity h and τ_{I,i^3} is the isospin wave function with total isospin I and third component i^3. Also, i^3_N and h_N are the isospin projection and helicity of the nucleon, respectively.

Assuming helicity conservation in the hard kernel of quark interactions,

$$H \approx \delta_{\alpha_1\alpha'_1}\delta_{\alpha_1\alpha'_1}\delta_{\beta_1,\beta_1}\delta_{\gamma_1,\gamma'_1}\delta_{\beta_2,\beta_2}\delta_{\gamma_2,\gamma'_2}\frac{f(\theta)}{s^4}, \quad \text{(C4)}$$

one obtains a rather simple relation for NN scattering amplitude in the form [35]

$$\langle cd|T|ab\rangle = Tr(M^{ac}M^{bd}), \quad \text{(C5)}$$

with

$$M^{i,j}_{\alpha,\alpha'} = C^i_{\alpha,\beta\gamma}C^j_{\alpha',\beta\gamma} + C^i_{\beta\alpha,\beta}C^j_{\beta\alpha',\beta} + C^i_{\beta\gamma\alpha}C^j_{\beta\gamma\alpha'}, \quad \text{(C6)}$$

where one sums over all the possible values of β and γ.

Using the above equations for the helicity amplitudes defined in Eq. (24) and normalized according to Eq. (24) [35] for $pp \to pp$ one obtains

$$\begin{aligned}\phi_1 &= \tfrac{1}{9}(31F(\theta,s)+31F(\pi-\theta,s))\\ \phi_3 &= \tfrac{1}{9}(14F(\theta,s)+17F(\pi-\theta,s))\\ \phi_4 &= -\tfrac{1}{9}(17F(\theta,s)+14F(\pi-\theta,s)),\end{aligned} \quad \text{(C7)}$$

and for $pn \to pn$ one obtains

$$\begin{aligned}\phi_1 &= \tfrac{1}{9}(14F(\theta,s)+17F(\pi-\theta,s))\\ \phi_3 &= \tfrac{1}{9}(22F(\theta,s)+25F(\pi-\theta,s))\\ \phi_4 &= \tfrac{1}{9}(8F(\theta,s)+8F(\pi-\theta,s)),\end{aligned} \quad \text{(C8)}$$

with $\phi_2 = \phi_5 = 0$ due to helicity conservation.

The above-described formalism gives an explicit form for calculation of the charge weighted NN amplitudes described in Sec. II B. For example Eq. (15) can be calculated by modifying Eq. (C5) in the following form:

$$Q^{N_a}_F\langle cd|T|ab\rangle = \sum_{\alpha,\alpha'} Q_\alpha M_{ac}(\alpha,\alpha')M_{bd}(\alpha',\alpha)), \quad \text{(C9)}$$

where Q_α is the charge of the quark α in $|e|$ units.

APPENDIX D: HELICITY AMPLITUDES OF TWO-NUCLEON BREAKUP REACTIONS OFF ^{3}He TARGET

Replacing QIM amplitudes in Eq. (18) by NN helicity amplitudes of Eq. (24) and using the antisymmetry of the ground state wave function with respect to the exchange of quantum numbers of any two nucleons one obtains the following expressions for the helicity amplitudes of two nucleon breakup reactions off the ^{3}He nucleus, $\langle\lambda_{1f},\lambda_{2f},\lambda_s|A|\lambda_\gamma,\lambda_A\rangle$. For a positive helicity photon,

$$\begin{aligned}
&\langle +,+,\lambda_s|A|+,\lambda_A\rangle \\
&= B\int\big[Q_F\phi_5\Psi^{\lambda_A}_{^3\mathrm{He}}(+,-,\lambda_s)+Q_F\phi_1\Psi^{\lambda_A}_{^3\mathrm{He}}(+,+,\lambda_s)\big]\times m_N\frac{d^2p_\perp}{(2\pi)^2}\\
&\langle +,-,\lambda_s|A|+,\lambda_A\rangle \\
&= B\int\big[\big(Q^{N_1}_F\phi_3+Q^{N_2}_F\phi_4\big)\Psi^{\lambda_A}_{^3\mathrm{He}}(+,-,\lambda_s) - Q_F\phi_5\Psi^{\lambda_A}_{^3\mathrm{He}}(+,+,\lambda_s)\big]m_N\frac{d^2p_\perp}{(2\pi)^2}\\
&\langle -,+,\lambda_s|A|+,\lambda_A\rangle \\
&= B\int\big[-\big(Q^{N_1}_F\phi_4+Q^{N_2}_F\phi_3\big)\Psi^{\lambda_A}_{^3\mathrm{He}}(+,-,\lambda_s) + Q_F\phi_5\Psi^{\lambda_A}_{^3\mathrm{He}}(+,+,\lambda_s)\big]m_N\frac{d^2p_\perp}{(2\pi)^2}\\
&\langle -,-,\lambda_s|A|+,\lambda_A\rangle \\
&= B\int\big[Q_F\phi_5\Psi^{\lambda_A}_{^3\mathrm{He}}(+,-,\lambda_s)+Q_F\phi_2\Psi^{\lambda_A}_{^3\mathrm{He}}(+,+,\lambda_s)\big]\times m_N\frac{d^2p_\perp}{(2\pi)^2},
\end{aligned} \quad \text{(D1)}$$

and for a negative helicity photon,

$$\begin{aligned}
&\langle +,+,\lambda_s|A|-,\lambda_A\rangle \\
&= -B\int\big[-Q_F\phi_5\Psi^{\lambda_A}_{^3\mathrm{He}}(-,+,\lambda_s) + Q_F\phi_2\Psi^{\lambda_A}_{^3\mathrm{He}}(-,-,\lambda_s)\big]m_N\frac{d^2p_\perp}{(2\pi)^2}\\
&\langle +,-,\lambda_s|A|-,\lambda_A\rangle \\
&= -B\int\big[-\big(Q^{N_1}_F\phi_4+Q^{N_2}_F\phi_3\big)\Psi^{\lambda_A}_{^3\mathrm{He}}(-,+,\lambda_s) - Q_F\phi_5\Psi^{\lambda_A}_{^3\mathrm{He}}(-,-,\lambda_s)\big]m_N\frac{d^2p_\perp}{(2\pi)^2}\\
&\langle -,+,\lambda_s|A|-,\lambda_A\rangle \\
&= -B\int\big[\big(Q^{N_1}_F\phi_3+Q^{N_2}_F\phi_4\big)\Psi^{\lambda_A}_{^3\mathrm{He}}(-,+,\lambda_s) + Q_F\phi_5\Psi^{\lambda_A}_{^3\mathrm{He}}(-,-,\lambda_s)\big]m_N\frac{d^2p_\perp}{(2\pi)^2}
\end{aligned}$$

$$\langle -,-,\lambda_s|A|-,\lambda_A\rangle = -B\int\Big[-Q_F\phi_5\Psi^{\lambda_A}_{^3\mathrm{He}}(-,+,\lambda_s) + Q_F\phi_1\Psi^{\lambda_A}_{^3\mathrm{He}}(-,-,\lambda_s)\Big]m_N\frac{d^2p_\perp}{(2\pi)^2}, \quad \text{(D2)}$$

where $B=\frac{ie\sqrt{2}(2\pi)^3}{\sqrt{2s'_{NN}}}$. Because the scattering process is considered in the "γ-NN" center of mass reference frame, where z direction is chosen opposite to the momentum of incoming photon, the bound nucleon helicity states correspond to the nucleon spin projections $\frac{1}{2}$ for positive and $-\frac{1}{2}$ for negative helicities.

[1] S. J. Brodsky and G. R. Farrar, Phys. Rev. Lett. **31**, 1153 (1973); Phys. Rev. D **11**, 1309 (1975).
[2] V. Matveev, R. M. Muradyan, and A. N. Tavkhelidze, Lett. Nuovo Cimento **7**, 719 (1973).
[3] S. J. Brodsky and B. T. Chertok, Phys. Rev. Lett. **37**, 269 (1976).
[4] R. J. Holt, Phys. Rev. C **41**, 2400 (1990).
[5] J. Napolitano *et al.*, Phys. Rev. Lett. **61**, 2530 (1988); S. J. Freedman *et al.*, Phys. Rev. C **48**, 1864 (1993).
[6] J. E. Belz *et al.*, Phys. Rev. Lett. **74**, 646 (1995).
[7] C. Bochna *et al.*, Phys. Rev. Lett. **81**, 4576 (1998).
[8] E. C. Schulte *et al.*, Phys. Rev. Lett. **87**, 102302 (2001).
[9] K. Wijesooriya *et al.* (Jeff. Lab Hall A Collaboration), Phys. Rev. Lett. **86**, 2975 (2001).
[10] E. C. Schulte *et al.*, Phys. Rev. C **66**, 042201 (2002).
[11] M. Mirazita *et al.* (CLAS Collaboration), Phys. Rev. C **70**, 014005 (2004).
[12] X. Jiang *et al.* (Jeff. Lab Hall A Collaboration), Phys. Rev. Lett. **98**, 182302 (2007).
[13] N. Isgur and C. H. Llewellyn Smith, Phys. Rev. Lett. **52**, 1080 (1984).
[14] A. Radyushkin, Acta Phys. Pol. B **15**, 403 (1984).
[15] G. R. Farrar, K. Huleihel, and H. Y. Zhang, Phys. Rev. Lett. **74**, 650 (1995).
[16] T. C. Brooks and L. J. Dixon, Phys. Rev. D **62**, 114021 (2000).
[17] S. J. Brodsky, AIP Conf. Proc. **792**, 279 (2005).
[18] S. J. Brodsky and J. R. Hiller, Phys. Rev. C **28**, 475 (1983).
[19] S. J. Brodsky and J. R. Hiller, Phys. Rev. C **30**, 412 (1984).
[20] V. Y. Grishina, L. A. Kondratyuk, W. Cassing, A. B. Kaidalov, E. De Sanctis, and P. Rossi, Eur. Phys. J. A **10**, 355 (2001).
[21] N. A. Khokhlov, V. A. Knyr, and V. G. Neudatchin, Phys. Rev. C **75**, 064001 (2007).
[22] L. L. Frankfurt, G. A. Miller, M. M. Sargsian, and M. I. Strikman, Phys. Rev. Lett. **84**, 3045 (2000).
[23] M. M. Sargsian, in *proceedings of the workshop on "Exclusive Processes at High Momentum Transfer," Newport News, Virginia, May 15–18, 2002*, edited by Anatoly Radyushkin and Paul Stoler (River Edge, World Scientific, 2002), pp. 369–376.
[24] V. Y. Grishina, L. A. Kondratyuk, W. Cassing, E. De Sanctis, M. Mirazita, F. Ronchetti, and P. Rossi, Eur. Phys. J. A **19**, 117 (2004).
[25] M. M. Sargsian, Phys. Lett. **B587**, 41 (2004).
[26] M. M. Sargsian, AIP Conf. Proc. **1056**, 287 (2008).
[27] S. J. Brodsky *et al.*, Phys. Lett. **B578**, 69 (2004).
[28] R. Gilman and E. Piasetzky (spokespersons), "Hard Photodisintegration of a Proton Pair," Jefferson Lab proposal, E-03-101, 2003.
[29] S. J. Brodsky, C. E. Carlson, and H. J. Lipkin, Phys. Rev. D **20**, 2278 (1979).
[30] L. L. Frankfurt and M. I. Strikman, Phys. Rep. **76**, 215 (1981).
[31] L. L. Frankfurt and M. I. Strikman, Phys. Rep. **160**, 235 (1988).
[32] A. Nogga, A. Kievsky, H. Kamada, W. Gloeckle, L. E. Marcucci, S. Rosati, and M. Viviani, Phys. Rev. C **67**, 034004 (2003).
[33] L. W. Mo and Y. S. Tsai, Rev. Mod. Phys. **41**, 205 (1969).
[34] C. G. White *et al.*, Phys. Rev. D **49**, 58 (1994).
[35] G. R. Farrar, S. Gottlieb, D. W. Sivers, and G. H. Thomas, Phys. Rev. D **20**, 202 (1979).
[36] M. Jacob and G. C. Wick, Ann. Phys. **7**, 404 (1959) [Ann. Phys. **281**, 774 (2000)].
[37] G. P. Ramsey and D. W. Sivers, Phys. Rev. D **45**, 79 (1992).
[38] J. M. Laget, Nucl. Phys. **A497**, 391C (1989).
[39] J. M. Laget, Phys. Lett. **B151**, 325 (1985).
[40] N. d'Hose *et al.*, Phys. Rev. Lett. **63**, 856 (1989).
[41] L. Machenil, M. Vanderhaeghen, J. Ryckebusch, and M. Waroquier, Phys. Lett. **B316**, 17 (1993).
[42] J. Ryckebusch, M. Vanderhaeghen, L. Machenil, and M. Waroquier, Nucl. Phys. **A568**, 828 (1994).
[43] C. Giusti and F. D. Pacati, Nucl. Phys. **A535**, 573 (1991).
[44] L. L. Frankfurt, M. M. Sargsian, and M. I. Strikman, Phys. Rev. C **56**, 1124 (1997).
[45] M. M. Sargsian, Int. J. Mod. Phys. E **10**, 405 (2001).
[46] W. R. Gibbs and B. Loiseau, Phys. Rev. C **50**, 2742 (1994).
[47] C. Granados, Ph.D. thesis (in progress).
[48] HEPDATA, The Durham HEP database, http://durpdg.dur.ac.uk/hepdata, 2008.
[49] R. J. Glauber, Phys. Rev. **100**, 242 (1955); in *Lectures in Theoretical Physics*, edited by W. Brittain and L. G. Dunham (Interscience, New York, 1959), Vol. 1.
[50] M. Sargsian and M. Strikman, Phys. Lett. **B639**, 223 (2006).